Feature Article

Polymer blends, copolymers and networks. Scattering properties and phase behavior

Mustapha Benmouna

Max-Planck-Institut für Polymerforschung, Postfach 3148, D-55021 Mainz, Germany

Robert Briber

University of Maryland, Department of Materials and Nuclear Engineering, 2100 Marie Mount Hall College Park, MD 20742, USA

*Boualem Hammouda**

National Institute of Standards and Technology, Building 235, E 151, Gaithersburg, MD 20899, USA

(Received: April 4, 1996; revised manuscript of June 10, 1996)

SUMMARY:

The phase behavior and scattering properties of polymer blends, copolymers and networks in solution and in bulk are examined. The theoretical framework used here is based upon the extension of the random phase approximation to polymers proposed by de Gennes and its application to chains with various architectures. The case of blends containing stiff chains is considered and the effect of nematic interaction on the phase behavior and scattering properties is discussed. The compressibility problem is reviewed in connection with the free volume theory models. The coupling between density and composition fluctuations is examined together with the effects of pressure on the structural and thermodynamic properties of blends. The dynamics of copolymers are also examined in the light of the new developments both from the theoretical and experimental fronts. The extent to which the chain architecture affects phase behavior, static scattering and dynamic behavior is discussed. A particular emphasis is put on the case of cyclic homopolymers and copolymers. Free chains in a network and crosslinked blends are also a subject of particular interest in this paper. The interplay between macrophase and microphase transitions due to the crosslinks and the electrostatic forces for charged polymers is also considered. De Gennes' analogy betwen the elastic restoring forces in the network and the Coulomb forces in the dielectric medium is generalized by including the screening phenomenon. This generalization is required in order to account for the experimental observations in the low momentum transfer range. Following Briber et al., it is argued that the new screening length can be related to the initial fluctuations at the temperature of crosslinking.

1. Introduction

The phase behavior and scattering properties of polymer blends, copolymers and crosslinked networks are the subject of intensive investigations both from the theoretical and the experimental points of view[1–14]. These studies are important for the understanding of the stability of polymer alloys and improvement of the perfor-

 CCC 1022-1344/97/$05.00

mance of material composites under stringent environmental conditions where these materials admit practical applications. Here, we review some of their fundamental aspects focussing essentially on conditions where there are weak fluctuations. We also consider the case where the systems undergo pressure forces which could induce important modifications in their phase behavior and structural and dynamic properties.

In most of the cases of interest here, models of linear response theory are useful in obtaining information related to the scattering and thermodynamic properties. For example, the static scattering technique is a basic tool for polymer characterization and provides precise measures of the molecular weight, index of polymerization, radius of gyration and second virial coefficient. These results are implemented through the classical Zimm plot analysis where the inverse scattered intensity is represented as a function of q^2 and c, where q is the amplitude of the wave vector and c is the concentration[15]. From a theoretical point of view, we shall rely in our description of the scattering properties and phase behavior of various systems on the random phase approximation (RPA) as first suggested by the Gennes[2] but with an extension to fit the kind of information one deals with and the system under investigation. The main assumption implicit in this procedure is to neglect the effect of fluctuations. Many experimental studies using different techniques such as static light scattering[16–18], quasi elastic light scattering[19–23] and neutron spin echo[24–26] have revealed that the RPA is a good first order approximation which accounts quite well for the qualitative behavior of data obtained from various systems involving homopolymers and copolymers of different architectures both in the bulk and in solution. This is true as long as the system remains stable and is not subject to strong fluctuations. Therefore, we keep our discussions at the level of the standard RPA introducing wherever required particular specific features for each problem under examination. One can readily within this procedure invoke a renormalization argument (i.e. first loop renormalization approximation) by assuming that certain important properties such as the interaction parameters or the excluded volume parameters and the friction coefficients are renormalized to include partly the effects of fluctuations.

On the other hand, it is sometimes more convenient to introduce molecular properties in order to avoid carrying out unnecessary constant factors which are irrelevant for the understanding of the qualitative trends. Examples of such properties are the degree of polymerization $N = M/m_0$, which is the ratio of the polymer and the monomer molecular weights; the volume fraction of the polymer φ is the ratio of the concentration c expressed in g/cm^3 and the polymer density ρ; the chain form factor $P(q)$ and the excluded volume parameter v

$$v = \frac{1}{\varphi_s} - 2\chi \tag{1}$$

where $\varphi_s = 1 - \varphi$ is the solvent volume fraction and χ the polymer-solvent interaction parameter. The static structure factor $S(q)$ is proportional to the scattered intensity $I(q)$

$$S(q) = I(q)/(\nu - \nu_s)^2 \tag{2}$$

where q is related to the wavelength of the incident radiation λ and the scattering angle θ by the usual relation $q = \frac{4\pi}{\lambda} \sin(\theta/2)$, $\nu - \nu_s$ is the contrast factor between the polymer and the solvent and is given by $\partial n/\partial c$, the increment of refractive index in the case of light scattering. Using Zimm's single contact approximation, one finds[27]:

$$\frac{1}{S(q)} = \frac{1}{N\varphi P(q)} + \frac{1}{\varphi_s} - 2\chi \tag{3}$$

This is a basic result derived long time ago by Zimm and used on a routine basis for the measurement of N, the radius of gyration R_g and χ. It has been extended to multicomponent polymer mixtures and to polymers of different architectures by various authors[1,9,28]. Some cases will be examined in the present paper. Likewise, quasi-elastic scattering techniques provide useful information on the dynamics of chains and relaxation processes either in dilute or strong solutions, or in bulk. The time evolution of the intermediate scattering function which is directly accessible in a dynamic scattering experiment $S(q, t)$ is given by the generalized Langevin equation[1,9]

$$\frac{\partial S(q,t)}{\partial t} + \Omega(q) S(q,t) - \int_0^t \mathrm{d}u\, \Theta(q,t) S(q,u) = 0 \tag{4}$$

where $\Omega(q)$ is the first cumulant and $\Theta(q, t)$ is the memory function. In the mean field approximation, one can neglect the memory function and assume that the decay of $S(q, t)$ is entirely described by the first cumulant $\Omega(q)$:

$$S(q, t) = S(q) \mathrm{e}^{-\Omega(q)t} \tag{5}$$

The first cumulant is usually defined in terms of a generalized mobility (Onsager coefficient) $M(q)$ and $S(q)$:

$$\Omega(q) = q^2 k_B T M(q) S^{-1}(q) \tag{6}$$

T is the absolute temperature, k_B Boltzmann's constant. $M(q)$ is a sum of the Rouse term and the hydrodynamic interaction term. The latter one is usually obtained from the Oseen tensor model and leads to the mode coupling function $f(x)$[9,29,30]:

$$M(q) = \frac{\varphi}{\zeta} + \frac{1}{4\pi^2 \eta} \int_0^\infty \mathrm{d}k f\left(\frac{q}{k}\right) S(k) \tag{7}$$

$$f(x) = x^2 \left[\frac{x^2 + 1}{2x} \ln \left| \frac{x+1}{x-1} \right| - 1 \right] \tag{8}$$

η is the viscosity of the solution and ζ the friction coefficient of a monomer of size σ:

$$\zeta = 6\pi\eta\sigma \tag{9}$$

In the short time limit, the relaxation of $S(q, t)$ is well described by Eq. (5) but in some cases memory effects are important and a strong deviation from the simple exponential decay is observed. For a single chain in a theta solvent, using Rouse normal mode analysis, de Gennes obtained[31]:

$$\frac{S(q,t)}{S(q)} = \int_0^\infty \mathrm{d}u\, \mathrm{e}^{[-u-g(u/\sqrt{\Omega t})]} \tag{10}$$

$$g(u) = \frac{2}{\pi}\int_0^\infty \mathrm{d}x \frac{\cos xu}{x^2}[1 - \mathrm{e}^{-x^2}] \tag{11}$$

$$\Omega(q) = \frac{k_\mathrm{B}T}{12\zeta\sigma^2}(q\sigma)^4 \tag{12}$$

Extending this normal mode analysis by including hydrodynamic interaction, Dubois-Violette and de Gennes obtained a different result[32]:

$$\frac{S(q,t)}{S(q)} = \int_0^\infty \mathrm{d}u\, \mathrm{e}^{[-u-(\Omega t)^{2/3}h[u(\Omega t)^{-2/3}]]} \tag{13}$$

$$h(u) = \frac{2}{\pi}\int_0^\infty \mathrm{d}x \frac{\cos xu}{x^2}\left[1 - \mathrm{e}^{-x^{3/2}/\sqrt{2}}\right] \tag{14}$$

$$\Omega(q) = \frac{k_\mathrm{B}T}{6\pi\eta}q^3 \tag{15}$$

These expressions are valid in the intermediate q and t ranges defined by $\sigma < q^{-1} < R_\mathrm{g}$ and $w^{-1} < t < (Dq^2)^{-1}$ where w is the monomer jump frequency and D the chain diffusion coefficient.

$$w = \frac{3k_\mathrm{B}T}{\zeta\sigma^2} \tag{16}$$

Pecora[33] and Akcasu et al.[34] calculated $S(q\ t)$ in a wider range of q and t values including $q \sim \sigma^{-1}$ and $t \sim (Dq^2)^{-1}$ using a somewhat different normal mode analysis

$$S(q,t) = \mathrm{e}^{-\nu_1 \frac{D_0}{N}q^2 t}\sum_{ik}\mathrm{e}^{-\frac{q^2\sigma^2}{6}\sum_l \mu_l^{-1}F_{ikl}(t)} \tag{17}$$

where the function $F_{ikl}(t)$ is given by:

$$F_{ikl}(t) = |Q_{il}|^2 + |Q_{kl}|^2 + 2\mathrm{Re}(Q_{il}Q_{kl})\,\mathrm{e}^{-w_0\mu_l\nu_l t} \tag{18}$$

Q_{ij} and μ_l are the eigenvectors and eigenvalues of the nearest neighbor interaction matrix. For open Gaussian chains, one has:

$$Q_{ij} = \left(\frac{2}{\pi}\right)^{1/2} \cos\left[\frac{\pi(j-1/2)(k-1)}{N}\right] \tag{19}$$

$$\mu_l = 4\sin^2\left(\frac{\pi l}{2N}\right) \tag{20}$$

The eigenvalues ν_l (l = 1, 2, ...) are all equal to 1 in the Rouse limit and this problem was first solved by Pecora. In the intermediate q-range ($\sigma \ll q^{-1} \ll R_g$) one obtains de Gennes' result in Eq. (10). In the presence of hydrodynamic interaction, the eigenvalues ν_l are calculated using the eigenvectors of cyclic polymers. For Gaussian unperturbed chains, one finds:

$$\nu_{l+1} = 1 + \frac{\zeta}{\sqrt{6\pi}\pi\eta\sigma} \sum_{n=1}^{N-1} \frac{\cos(2\pi nl/N)}{\sqrt{n(1-n/N)}} \tag{21}$$

These results were used extensively in the literature for the interpretation of quasi-elastic light and neutron spin echo measurements obtained on differents systems and in particular on binary polymer/solvent solutions[34-36] ternary mixtures of two polymers and a solvent[24,37-39] and blends. In the small q range where $qR_g \ll 1$, one obtains a diffusive process for which

$$\frac{S(q,t)}{S(q)} = \mathrm{e}^{-q^2Dt} \tag{22}$$

where, in the Rouse limit $D = D_0/N$ and in the presence of hydrodynamic interaction one may express D in terms of the hydrodynamic radius R_h by writing:

$$D = k_B T/(6\pi\eta R_h) \tag{23}$$

$$R_h \approx N^{1/2}\,\sigma \tag{24}$$

In the intermediate ranges of q and t defined earlier, one observes the shape function derived directly by de Gennes and Dubois-Violette[31,32] using the normal mode method. In the short time and high q limits, the diffusional process of a single monomer is recovered:

$$S(q,t) = \mathrm{e}^{-q^2\frac{k_B T}{\zeta}t} \tag{25}$$

In the intermediate q range and at long times, the results of Akcasu, Pecora, de Gennes and Dubois-Violette lead to the same result which, in the Rouse limit, reads

$$\frac{S(q,t)}{S(q)} \longrightarrow e^{-(\Omega_R t)^{1/2}} \tag{26}$$

whereas in the presence of hydrodynamic interaction, one finds:

$$\frac{S(q,t)}{S(q)} \longrightarrow e^{-(\Omega_Z t)^{2/3}} \tag{27}$$

The scaling frequencies Ω_R and Ω_Z are given by Eqs. (12) and (15), respectively.

These results concern single chain properties in theta solvent conditions. Nevertheless, they are found useful even beyond these conditions where they are applied successfully to data where not only excluded volume interaction is present but also interactions between chains of different species. They are also used to analyze reptation of chains in the bulk. Therefore, the above results of $S(q, t)$ can be used as the bare dynamic scattering functions in the generalization of the random phase approximation (RPA) to dynamical properties. These applications will be discussed in more detail later in this paper.

Another problem which is considered in this paper deals with the effects of crosslinking. It is known that crosslinking produces strong effects on the phase behavior and scattering properties of blends. In general it induces enhancement of compatibility towards macrophase separation but it may give rise to a microphase separation transition. This modification of the nature of the phase transition upon crosslinking was examined by de Gennes[40] who proposed an analogy with the polarization of charges in a dielectric medium. The model of de Gennes predicts a peak in the scattering intensity and this prediction is consistent with the experimental observation. However, unlike the experiment, the model predicts a zero scattering at[14] $q = 0$. This prompted a correction of the model using a similar analogy with the charges in a dielectric medium but including the effect of screening. The screening length is identified with the correlation length describing the range of fluctuations existing at the moment of crosslinking[41,42].

2. Blends and copolymers: bulk and solution

Eq. (3) gives the structure factor in the case of a polymer/solvent solution. If one assumes that the solvent in this binary mixture has a finite size or can be considered as a polymer whose properties are designated with a subscript B, then Eq. (3) can be written in a slightly different form

$$\frac{1}{S(q)} = \frac{1}{N_A \varphi_A P_A(q)} + \frac{1}{N_B \varphi_B P_B(q)} - 2\chi \tag{28}$$

where N_B is the degree of polymerization and $P_B(q)$ the form factor of B, and the properties of the other polymer are indicated by the subscript A. The interaction

parameter between A and B is denoted χ. This is the case of an incompressible blend where one has

$$\varphi_A = 1 - \varphi_B \qquad S_{AA}(q) = S_{BB}(q) = -S_{AB}(q) = S(q) \tag{29}$$

Eq. (28) is the classical result obtained by de Gennes using the RPA. Here it has been deduced from Zimm's single contact approximation (SCA) implying that the SCA and the RPA belong to the same class of approximations[1)].

If the two polymers A and B are connected together and form a diblock copolymer, one obtains Leibler's result[10)]

$$\frac{1}{S(q)} = \frac{(N_A + N_B)(P_A + P_B + 2P_{AB})}{\varphi_A \varphi_B N_A N_B (P_A P_B - P_{AB}^2)} - 2\chi \tag{30}$$

where P_{AB} is a form factor characteristic of the copolymer architecture and can be obtained from the geometric relationship between P_A, P_B and P_T; P_T is the total form factor of the copolymer:

$$P_T = f^2 P_A + (1-f)^2 P_B + 2f(1-f) P_{AB} \tag{31}$$

f is the composition of the copolymer in monomer A:

$$f = N_A/(N_A + N_B) \tag{32}$$

All these form factors are normalized to 1 at $q = 0$ and hence $S(q = 0) = 0$ regardless of the interaction parameter. Within this RPA result the variation of $S(q)$ presents a maximum at $q^* \approx 2/R_g$ where R_g is the radius of gyration, also regardless of the interaction parameter. However, the height of the maximum increases with χ. One could improve the RPA by allowing R_g to be a function of χ as suggested by computer simulations. The interaction parameter can reach a high value by changing the temperture in such a way that the scattering intensity diverges. When this critical value is reached, the system undergoes microphase separation transition (MST) or order-disorder transition (ODT). When this transition takes place, the RPA breaks down and one should resort to more sophisticated methods to describe the properties of the phase separated regions in the medium. The plain RPA and its renormalized versions constitute a first order approximation for the description of the scattering behavior in the one phase region and eventually, it could be used to predict approximately the critical conditions for macro- and microphase separation transitions.

Eqs. (28) and (30) are classical results which turn out to be extremely useful for experimentalists. These equations were and are still extensively used to get an estimate of the effective interaction parameter between monomer species belonging to blends or to block copolymers.

In the case of a ternary mixture of homopolymer A, homopolymer B and a solvent, the scattering intensity is obtained within the RPA[1,43)]:

$$I(q) = \frac{a^2 S_A^0 + b^2 S_B^0 + (a^2 v_B + b^2 v_A - 2ab v_{AB}) S_A^0 S_B^0}{1 + v_A S_A^0 + v_B S_B^0 + (v_A v_B - v_{AB}^2) S_A^0 S_B^0} \tag{33}$$

$$S_A^0(q) = \varphi_A N_A P_A(q) \tag{34}$$

$$S_B^0(q) = \varphi_B N_B P_B(q) \tag{35}$$

This result has been extensively used by experimentalists to analyze light scattering data obtained from various ternary mixtures of two polymers and a low molecular weight solvent. It predicts the correct trends in various different systems, and in many cases even a quantitative agreement is observed between data and theory[16–18]. It is worthwhile to recall that the limit of Eq. (33) at $q = 0$ which describes the forward scattering intensity has been derived long time ago by Stockmayer[44] as a special case of multicomponent polymer mixtures in solution using pure thermodynamic arguments. His result was the theoretical basis for the analysis of thermodynamic scattering data for ternary mixtures until its generalization to finite q by Benoit et al.[1,43]

If in addition to the two homopolymers A and B, a copolymer AB is present in the mixture, the above result is slightly modified and the scattered intensity becomes[1,43,45]:

$$I(q) = \frac{a^2 S_A^0 + b^2 S_B^0 + 2ab S_{AB}^0 + (a^2 v_B + b^2 v_A - 2ab v_{AB})(S_A^0 S_B^0 - S_{AB}^{02})}{1 + v_A S_A^0 + v_B S_B^0 + 2 v_{AB} S_{AB}^0 + (v_A v_B - v_{AB}^2)(S_A^0 S_B^0 - S_{AB}^{02})} \tag{36}$$

$$S_A^0(q) = \varphi_{AH} N_{AH} P_{AH}(q) + \varphi_{AC} N_{AC} P_{AC}(q) \tag{37}$$

$$S_B^0(q) = \varphi_{BH} N_{BH} P_{BH}(q) + \varphi_{BC} N_{BC} P_{BC}(q) \tag{38}$$

$$S_{AB}^0(q) = [\varphi_{AC} N_{AC} \varphi_{BC} N_{BC}]^{1/2} P_{ABC}(q) \tag{39}$$

The subscripts H and C refer to homopolymers and copolymers, respectively. This result contains both the cases of solution and bulk. In the absence of solvent, for an incompressible mixture, one has $\frac{(a-b)^2}{I(q)} = \frac{1}{S(q)}$ the same result as in Eq. (30) but the bare structure factors given by Eqs. (37) to (39).

Eq. (36) was used by Duval et al.[46] to analyze neutron scattering data on copolymers made of two equal blocks of deuterated and ordinary polystyrene (PS) in a mixture of deuterated and ordinary toluene at several polymer concentrations. Hashimoto et al.[47] also used the same equation to examine X-ray data for diblock copolymers of polystyrene and polyisoprene (PI) in dioctyl phthalate (DOP) for two compositions (50 and 60%) and different temperatures approaching quite close the critical temperature for the microphase separation transition. In the latter study, the authors used both Eqs. (36) and (28) where they introduced the concept of effective contrast and interaction parameter. Their main conclusion is that Eq. (36) provides a

reasonable description of the data especially for symmetric diblocks where the zero average contrast condition is fulfilled[48].

2.1. *Liquid crystalline behavior of stiff polymers*

The generalization of these results to multicomponent polymer mixtures including stiff chains has been presented by several authors[49–51] Hammouda[51,52] developed the general formalism for the static scattering properties using the RPA. In addition to the enthalpic interaction governing the mixing and demixing of different species, one introduces other interactions due to angular correlations (monomer orientations) which can give rise to other types of phase transitions. Such interactions can be nematic, smectic, discotic etc. We limit our considerations to the case of the nematic interaction where one writes the interaction potential between a pair of monomers with the orientations u' and u'' as:

$$w(u'\,u'') = w_0 - w_1\,(u'u' - \mathrm{I}/3) : (u''u'' - \mathrm{I}/3) \tag{40}$$

The first term w_0 is isotropic and is independent of the orientations. The second is anisotropic and corresponds to the nematic interaction. The Maier-Saupe interaction parameter w_1 is sensitive to the monomer orientations. For multicomponent mixtures, the interaction parameters become matrices:

$$w(u', u'') = w_0 - w_1\,(u'u' - \mathrm{I}/3) : (u''u'' - \mathrm{I}/3) \tag{41}$$

The scattering formalism for these mixtures has been worked out by several authors[51–55] on the basis of an extension of the RPA to include the effect of chain stiffness. Here we follow the notations and procedure of Hammouda[51,52]:

$$S = [\mathrm{I} + S_0 w_0 + (2/3)R_0^{\mathrm{T}} w_1 M^{-1} R_0 w_0]^{-1}[S_0 + (2/3)R_0^{\mathrm{T}} w_1 M^{-1} R_0] \tag{42}$$

where $M = \mathrm{I} - 2\,T_0\,w_1/3$; R_0, R and T_0 are given by:

$$S_0(q) = \int \mathrm{d}u \int \mathrm{d}u'\, S_0(q, u, u') \tag{43}$$

$$S(q) = \int \mathrm{d}u \int \mathrm{d}u'\, S(q, u, u') \tag{44}$$

$$R_0(q) = \frac{3}{2} \int \mathrm{d}u \int \mathrm{d}u'\, S_0(q, u, u')[(q \cdot u)^2 - 1/3] \tag{45}$$

$$R(q) = \frac{3}{2} \int \mathrm{d}u \int \mathrm{d}u'\, S(q, u, u')[(q \cdot u)^2 - 1/3] \tag{46}$$

$$T_0(q) = \frac{9}{4} \int \mathrm{d}u \int \mathrm{d}u'\, S_0(q, u, u')[(q \cdot u)^2 - 1/3][(q \cdot u')^2 - 1/3] \tag{47}$$

A simple and useful application of these results is a blend of flexible chains A and rigid rods B. In this case, Eq. (42) to (47) give:

$$S(q) = \frac{I(q)}{(a-b)^2}$$

$$= \frac{2(R_B^0)^2 w_B^1 S_A^0/3 + (1 - 2T_B^0 w_B^1/3) S_A^0 S_B^0}{2(R_B^0)^2 w_B^1 (1 - 2\chi S_A^0)/3 + (S_A^0 + S_B^0 - 2\chi S_A^0 S_B^0)(1 + 2T_B^0 w_B^1/3)} \tag{48}$$

$$S_A^0(q) = \varphi_A N_A P_A(q) \tag{49}$$

$$\frac{S_B^0}{\varphi_B N_B} = \int_0^1 \mathrm{d}x j_0^2\left(x\frac{qbN_B}{2}\right) \tag{50}$$

$$\frac{R_B^0}{\varphi_B N_B} = \frac{3}{2}\int_0^1 \mathrm{d}x\left(x^2 - \frac{1}{3}\right) j_0^2\left(x\frac{qbN_B}{2}\right) \tag{51}$$

$$\frac{T_B^0}{\varphi_B N_B} = \frac{9}{4}\int_0^1 \mathrm{d}x\left(x^2 - \frac{1}{3}\right)^2 j_0^2\left(\frac{qbN_B}{2}\right) \tag{52}$$

where $j_0(\ldots)$ is the zeroth order Bessel function.

If one has a diblock copolymer AB in which block A is flexible and B is rigid, the structure factor becomes:

$$S(q) = \frac{2w_B^1 R/3 + T\Delta S}{(S_T + 2\chi\Delta S)T + 2(w_B^1 R' - 2\chi w_B^1 R)/3} \tag{53}$$

$$R = R_B^{02} S_A^0 - 2R_{AB}^0 R_B^0 S_{AB}^0 + R_{BA}^{02} S_B^0 \tag{54}$$

$$T = 1 - 2T_B^0 w_B^{1/3} \tag{55}$$

$$\Delta S = S_A^0 S_B^0 - S_{AB}^{02} \tag{56}$$

$$S_T = S_A^0 + S_B^0 + 2S_{AB}^0 \tag{57}$$

$$R' = R_B^{02} + R_{AB}^{02} + 2R_{AB}^0 R_B^0 \tag{58}$$

Wagner et al.[56] reported small-angle neutron scattering (SANS) data on solutions of poly(benzyl L-glutamate) (PBLG) in deuterated dimethylformamide (*d*-DMF) in a wide range of concentrations. They analyzed their results using the modified RPA described above and observed a good agreement between data and theoretical predictions showing once more the wide range of applications of the RPA and its usefulness to experimentalists.

2.2. *Effects of pressure*

Hammouda and Bauer[57] studied blends of deuterated polystyrene (dPS) and polyvinylmethylethylene (PVME) as a function of pressure, temperature and composition using small angle neutron scattering. They observed that $\chi(T, P)$ has a strong pressure dependence. They have also noticed that such dependence is not modified by the blend composition which led to the conclusion that compressibility is not the reason for the variation of the interaction parameter with composition as suggested earlier. Hammouda and Bauer observed that χ follows the temperature dependence

$$\chi(T, P) = A(P)/T + B(P) \tag{59}$$

where both A and B are quite senstive to P. Applying pressure to the blend results in damping of fluctuations and shifts the spinodal curve. Janssen et al.[58] also studied blends of dPS/PVME by SANS and came to the conclusion that $B(P)$, the entropic contribution to the interaction parameter, is strongly pressure dependent whereas the enthalpic term A is not sensitive to P.

The effects of pressure were also studied on block-copolymers. Hadjuk et al.[59] performed a small angle X-ray scattering study on PS-polyisoprene (PI) diblock copolymer and observed an increase of the ODT (order-disorder transition) temperature. Hammouda et al.[60] considered diblock coolymers of PS-PI in dioctyl phthalate (DOP) using SANS. DOP was used to lower the glass transition temperature T_g of the copolymer below the ODT temperature and to eliminate possible interferences between the effects of T_g and T_{ODT}.

If a blend is compressible, the RPA fails to describe properly the scattering behavior under pressure effects. This approximation has been extended to compressible blends by various authors assuming that the monomer-monomer interaction potentials w_{aa} and w_{bb} are deduced from the *PVT* data of pure components. The compressible RPA version introduces the free volume as an additional component and its fraction is estimated from an equation of state. A scheme for analyzing the SANS data as a function of pressure starting from the RPA equations for a ternary incompressible mixture made of polymer species A and B and voids has been suggested. Indicating the voids parameters by a subscript 0, the results are[61]

$$S_{AA}(q) = \frac{S_A^0(1 + \nu_B S_B^0)}{1 + \nu_A S_A^0 + \nu_B S_B^0 + (\nu_A \nu_B - \nu_{AB}^2) S_A^0 S_B^0} \tag{60}$$

$$S_{BB}(q) = \frac{S_B^0(1 + \nu_A S_A^0)}{1 + \nu_A S_A^0 + \nu_B S_B^0 + (\nu_A \nu_B - \nu_{AB}^2) S_A^0 S_B^0} \tag{61}$$

$$S_{AB}(q) = \frac{-\nu_{AB} S_A^0 S_B^0}{1 + \nu_A S_A^0 + \nu_B S_B^0 + (\nu_A \nu_B - \nu_{AB}^2) S_A^0 S_B^0} \tag{62}$$

where the void properties enter through the excluded volume interaction parameters ν_A, ν_B and ν_{AB}:

$$\nu_A = \frac{1}{S_0} - \frac{2P_A^*}{k_B T} + C_A \tag{63}$$

$$\nu_B = \frac{1}{S_0} - \frac{2P_B^*}{k_B T} + C_B \tag{64}$$

$$\nu_{AB} = \frac{1}{S_0} - \frac{2P_{AB}^*}{k_B T} + C_{AB} \tag{65}$$

S_0 is the bare structure factor related to the void volume fraction f_0, the P^*'s are the cohesive energy densities or internal pressures and the C's are

$$C_A = -\frac{2\varphi_B}{(1-f_0)^2}(\ln f_0 + 1 - f_0)\left(\frac{P_A^*}{k_B T_A^*} - \frac{P_B^*}{k_B T_B^*}\right) \tag{66}$$

$$C_B = -\frac{2\varphi_A}{(1-f_0)^2}(\ln f_0 + 1 - f_0)\left(\frac{P_A^*}{k_B T_A^*} - \frac{P_B^*}{k_B T_B^*}\right) \tag{67}$$

$$C_{AB} = -\frac{(\varphi_A - \varphi_B)}{(1-f_0)^2}(\ln f_0 + 1 - f_0)\left(\frac{P_A^*}{k_B T_A^*} - \frac{P_B^*}{k_B T_B^*}\right) \tag{68}$$

The characteristic pressures and temperatures P_A^*, P_B^* and T_A^*, T_B^* are tabulated for different polymers. The free volume fraction f_0 is deduced from an equation of state such as the Sanchez-Lacombe equation[62,63]

$$(1-f_0)^2 + P/P^* + [\ln f_0 + 1 - f_0]T/T^* = 0 \tag{69}$$

where the quantity $\varphi_A/N_A + \varphi_B/N_B$ is neglected as compared to 1. More details on this procedure and its applications to the analysis of SANS data can be found elsewhere[61].

2.3. *Compressibility*

Benoit[1,64] has shown that in multicomponent polymer mixtures, the forward scattering intensity $I(q = 0)$ can be written as a sum of two terms. One is due to density

fluctuations and describes the compressibility of the mixture whereas the other term is due to composition fluctuations. He wrote

$$I(q=0) = V(a/v_0)^2 k_B T\beta + N_T k_B T[a^T][S]^{-1}[a] \tag{70}$$

where (a/v_0) is the scattering length per unit volume of solvent, v_0 being the molar volume of solvent, V the total volume of the sample, N_T the total number of particles or total number of lattice sites in the Flory-Huggins lattice, $N_T = V/v_0$, β is the isothermal compressibility coefficient:

$$\beta = \frac{v_0^2}{V} \frac{1}{(\partial\mu_0/\partial N_T)_P} = -\frac{1}{v}\left(\frac{\partial v}{\partial P}\right)_T \tag{71}$$

The elements of the matrix $[S]$ are given by the derivatives of the free energy per unit volume:

$$[S_{ij}]^{-1} = \frac{\partial^2 g}{\partial\varphi_i \partial\varphi_j} \tag{72}$$

$[a]$ is a column vector of contrast factors. Eq. (70) shows that in the forward scattering direction at $p = 0$, there is no coupling between density and composition fluctuations in multicomponent polymer mixtures. A similar expression was derived before by des Cloizeaux and Jannink[13,65]. In the case of a binary mixture polymer + solvent, Eq. (70) becomes

$$I(q=0) = (a_A N_A + a_B N_B)^2 k_B T\beta/V + N_A N_B (a_B v_A - a_B v_B)^2 k_B T(\partial\mu_A \partial N_B)^{-1} \tag{73}$$

$$I(q=0) = N_T \rho_A \langle a\rangle^2 k_B T\beta - v_A^2 v_B^2 \rho_A \rho_B (a_B/v_B - a_A/v_A)^2 k_B T(\partial\mu_A/\partial N_B)^{-1} \tag{74}$$

where $N_T = N_A + N_B$, $\rho A = N_A/V$ and $\rho_B = N_B/V$ are the mean number densities of the two species in the mixture. the extension of this formalism to finite q's has not been worked out yet. It could be also useful to write the counterpart equation for the time dependent scattering as probed by quasielastic light scattering or neutron spin echo technique.

One observes that in Eq. (74) neither the degree of polymerization nor the interaction parameter appear explicitly. One may assume that they are implicit in the quantities V_A/v_0 and $\partial\varphi_A/\partial N_B$. Since the thermodynamic analysis of Benoit is general, it would be useful to compare it with the method of scattering theory. Consider the earlier result for a ternary mixture with two polymers A and B and a slvent and replace mentally the solvent by voids. The scattering intensity is written as:

$$I(q) = (a-s)^2 S_{AA}(q) + (b-s)^2 S_{BB}(q) + 2(a-s)(b-s)S_{AB}(q) \tag{75}$$

Introducting x, the mean composition of the blend, and the new concentration variables $c_T(q)$ and $c_I(q)$

$$c_T(q) = c_A(q) + c_B(q) \tag{76}$$

$$c_I(q) = (1-x)c_A(q) - xc_B(q) \tag{77}$$

one can show that $I(q)$ can be written in the form:

$$I(q) = [(a-s)x + (b-s)(1-x)]^2 S_{CC}(q) + (a-b)^2 S_{XX}(q)$$

$$+2[(a-s)x + (b-s)(1-x)](a-b)S_{XC}(q) \tag{78}$$

$$\langle |c_T(q)|^2 \rangle = S_{CC}(q) = S_{AA}(q) + S_{BB}(q) + 2S_{AB}(q) \tag{79}$$

$$\langle |c_I(q)|^2 \rangle = S_{XX}(q) = (1-x)^2 S_{AA}(q) + x^2 S_{BB}(q) - 2x(1-x)S_{AB}(q) \tag{80}$$

$$\langle c_T(q)c_X(-q) \rangle = S_{XC}(q) = (1-x)[S_{AA}(q) + S_{AB}(q)] - x[S_{BB}(q) + S_{AB}(q)] \tag{81}$$

$S_{CC}(q)$ reflects the total concentration fluctuations, $S_{XX}(q)$ describes the composition fluctuations and $S_{XC}(q)$ the coupling between them. Starting from the RPA result[1)]

$$S^{-1}(q) = S_0^{-1}(q) + v \tag{82}$$

one can obtain the explicit form of the partial structure factors $S_{AA}(q)$, $S_{BB}(q)$ and $S_{AB}(q)$ in terms of the bare structure factors:

$$S_{AA}(q)^{-1} = S_A^0(q)^{-1} + \varphi_S^{-1} - 2\chi_{AS} - \frac{(\varphi_S^{-1} - \chi_{AS} - \chi_{BS} + \chi)^2}{S_B^0(q)^{-1} + \varphi_S^{-1} - 2\chi_{BS}} \tag{83}$$

$$S_{BB}(q)^{-1} = S_B^0(q)^{-1} + \varphi_S^{-1} - 2\chi_{BS} - \frac{(\varphi_S^{-1} - \chi_{AS} - \chi_{BS} + \chi)^2}{S_A^0(q)^{-1} + \varphi_S^{-1} - 2\chi_{AS}} \tag{84}$$

$S_{AB}(q) =$

$$\frac{-(\varphi_S^{-1} - \chi_{AS} - \chi_{BS} + \chi)}{(S_A^0(q)^{-1} + \varphi_S^{-1} - 2\chi_{AS})(S_B^0(q)^{-1} + \varphi_S^{-1} - 2\chi_{BS}) - (\varphi_S^{-1} - \chi_{AS} - \chi_{BS} + \chi)^2} \tag{85}$$

$S_{CC}(q)$, $S_{XX}(q)$ and $S_{XC}(q)$ are immediately deduced by combining Eqs. (78) to (85). Let us consider the conditions under which the coupling term vanishes. One has:

$$S_{XC}(q) =$$

$$\frac{(1-x)S_B^0(q)^{-1} - xS_A^0(q)^{-1} + \chi_{AS} - \chi_{BS} + (2x-1)\chi}{(S_A^0(q)^{-1} + \varphi_S^{-1} - 2\chi_{AS})(S_B^0(q)^{-1} + \varphi_S^{-1} - 2\chi_{BS}) - (\varphi_S^{-1} - \chi_{AS} - \chi_{BS} + \chi)^2} \tag{86}$$

If the degrees of polymerization are 1, noting that S_A^0 $(q = 0) = x\varphi_T$ and S_B^0 $(q = 0)$ $= (1 - x)$ φ_T, one finds that S_{XC} $(q = 0)$ is proportional to $\chi_{AS} - \chi_{BS} + (2x - 1)$ which is zero only if $\chi_{AS} = \chi_{BS}$ and either $\chi = 0$ or $x = 1/2$ or both. A similar observation can be made if one replaces the solvent by free volume. This analysis reduces to applying the standard RPA to compressible blends and accounts for the compressibility through "solvent free volume". This is consistent with Benoit's equation but it is not limited to the thermodynamic limit and applies to finite q. The problem which remains to be elucidated is whether the uncoupling between density and concentration fluctuations is general for a multicomponent mixture and at any q or must be applied only under specific conditions.

2.4. Dynamics of block copolymers

The dynamics of block copolymers has been investigated by various authors. One of the early investigations of this subject using the RPA is due to Akcasu and coworkers[66]. The single chain dynamics and the dynamics of semidilute and concentrated solutions of copolymers was reported later[67,68]. The scattering from a pure block copolymer is dominated by the structural mode. In the q range much higher than the inverse radius of gyration, the radiation probes the local dynamics of the chain and one observes internal modes which are similar to the ones observed in homopolymers. One has Rouse modes if hydrodynamic interaction is not included whereby the relaxation frequency Γ behaves as $q^{-2/\nu}$. Assuming the flory exponent ν $= 1/2$, it gives q^{-4} in the absence of excluded volume interaction and $q^{-3.66}$ otherwise. Should the hydrodynamic interaction be included, one finds that the relaxation frequency of the internal mode varies as q^{-3} whether excluded volume interaction is important or not. Such interaction introduces only a modification in the numerical factor in front of the expression of $\Gamma(q)$. As the probe scans the lower q range, one observes an entirely different behavior whether one deals with homopolymers or block copolymers. For homopolymers, one finds a diffusive mechanism whereby the relaxation frequency varies as $\Gamma = Dq^2$ and D is the diffusion coefficient of the chains. For copolymers, the relaxation is not diffusive since Γ has a finite limit at q $= 0$. This behvior is also encountered in polyelectrolytes where it is known as the plasmon mode[69,70]. The plasmon mode is attributed to the relaxation of counterions in the vicinity of polyions as if they were linked together. Likewise, in the case of a copolymer, when the block A moves, it pulls the block B with it and, therefore the relative relaxation of A and B blocks on the same chain gives rise to the structural mode of the copolymer for which the frequency Γ is constant when $q = 0$. This behavior has been predicted by Akcasu et al.[66] for block copolymers in the bulk and in solution[67]. The first experimental obervation of this structural mode was made by

Borsali et al. using NSE (neutron spin echo), on diblock copolymers of dPS-PS in toluene[25,26] and QELS (quasi-elastic light scattering) on PS-PMMA in toluene[71]. In the former case, a mixture of deuterated and ordinary toluene was used as a solvent in order to achieve the zero average contrast condition. The single mode observed in this experiment was identified as the structural mode in accordance with the theoretical prediction of RPA. For the PS-PMMA diblock in toluene investigated by QELS, two modes were found. The amplitudes and frequencies of these modes were analyzed within the theoretical framework and a complete agreement was found with regard to the identification of the modes, i.e., the cooperative mode corresponding to the relaxation of the total concentration fluctuations as in the case of homopolymers. The second mode was identified as the structural mode and has similar characteristics as the mode observed in the bulk state. Haida, Duval et al.[72] investigated the dynamics of similar systems and found slightly different results. They were not able to observe the structural mode characteristic of the internal architecture of the copolymer. They observed nonetheless two modes. The fast mode corresponds to the diffusion of the chain as a whole and the slow mode represents the diffusion of copolymer micelles. Jian et al.[73] and Pan et al.[74] performed QELS studies of various block copolymers in semidilute and concentrated solutions and found the overall diffusion mode, the micellar mode and a third mode which is attributed to the composition polydispersity. This new mode is found to behave as the structural mode of the copolymer in that its relxation frequency has a constant value at $q = 0$. We shall come back to this problem in the following section where the case of cyclic copolymers and homopolymers is considered and their dynamical properties compared with the linear chain systems.

3. The case of cyclic homopolymers and copolymers

In the preceeding section, we have examined the effects of rigidity by considering briefly the scattering from mixtures of flexible and rigid homopolymers and diblock copolymers made of a flexible and a rigid block. Here in this section, as a special case of the effects of chain architecture on the scattering and phase behavior of polymer mixtures we would like to examine another case of mixtures with different architecture by analyzing the behavior of cyclic polymers and compare their behavior with the one observed in the counterpart mixtures made of linear polymers. The interest on cyclic polymers is not new and started in the late fifties when it was recognized that certain biological macromolecules such as DNA and certain polypeptides have a cyclic conformation[75]. Moreover, the case of cyclic chains leads to a substantial simplification in some fundamental studies of chain conformations because it introduces cyclic boundary conditions and avoids complications due to chain end effects. These effects may be important, especially for relatively short chains where any point along the chain is not far from the ends and the correlations between an interior point and an end point are substantially different from the correlations between two interior points. In recent years, a growing interest has been put on cyclic polymers due to the developments of new techniques both on the experimental and the theoretical fronts. The progress in polymer synthetic chemistry of

long cyclic homopolymers and copolymers, together with the deuteration technique and the developments in the SANS, NSE and QELS techniques has opened up new prospectives for understanding the thermodynamic, structural and dynamical properties of these systems. Recently, a number of experimental studies have been reported on cyclic homopolymers and copolymers. For example, Santore et al.[76] performed a comparative study of the thermodynamic stability and phase separation kinetics of polymer blends containing cyclic chains of high molecular weight. They considered two blends of PS/PVME, one containing only linear chains and the other containing a certain percentage of cyclic PS chains. They measured the cloud point temperatur over a wide range of composition and found that the blend containing cyclic polymers phase separates at a temperature roughly 7 °C above the cloud point of the system with linear chains only. It should be noted that the blend PS/PVME admits a LCST (lower critical solution temperature). More recently, Amis et al.[77,78] reported elastic and quasielastic light scattering data on cyclic diblock copolymers of PS-PDMS (polydimethylsiloxane) in cyclohexane and linear triblock copolymers of PDMS-PS-PDMS in cyclohexane. The two systems were studied in similar conditions of molecular weight, composition, concentration and temperature. The results were compared in order to investigate the effects of cyclic architecture of the copolymer on the structural and dynamical properties in the dilute range and in a wide domain of temperature. It is interesting to note that only the PS block which is about 1/3 of the whole copolymer is visible to the light since PDMS and cyclohexane have roughly the same index of refraction. Moreover, the theta temperature of PS in cyclohexane is 35 °C and the range of temperature investigated is between 35 °C and 12 °C. The main results of the static measurements were that the apparent theta temperature for the linear copolymer was about 20 °C whereas for the cyclic copolymer, cyclohexane behaved as a good solvent even at the lowest temperature investigated which was 12 °C. The QELS measurements revealed that the dynamic correlation function showed a single diffusive mode between 35 °C and 20 °C for both copolymers. For the linear copolymer, the dynamic correlation function showed a multimodal behavior below 20 °C. At 20 °C, a second slow diffusive mode appeared indicating a beginning of copolymer micelle formation. For the cyclic copolymer, a single decay mode was observed from 35 °C through 12 °C, the lowest temperature investigated. These observations prompted a theoretical study of the static and dynamic properties of cyclic and linear polymers and copolymers which is briefly reviewed in the following section[79,80]. We consider the two systems illustrated in Figs. 1 and 2. The copolymer in Fig. 1 is similar to the one investigated by Amis et al. Blocks A

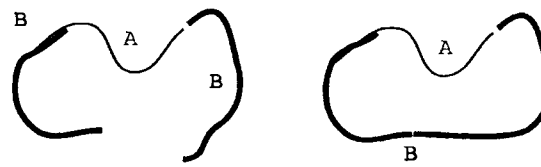

Fig. 1. Schematic representation of the linear triblock copolymer and cyclic diblock copoymer investigated by light scattering in ref.[78] and considered here as an application of the theoretical model

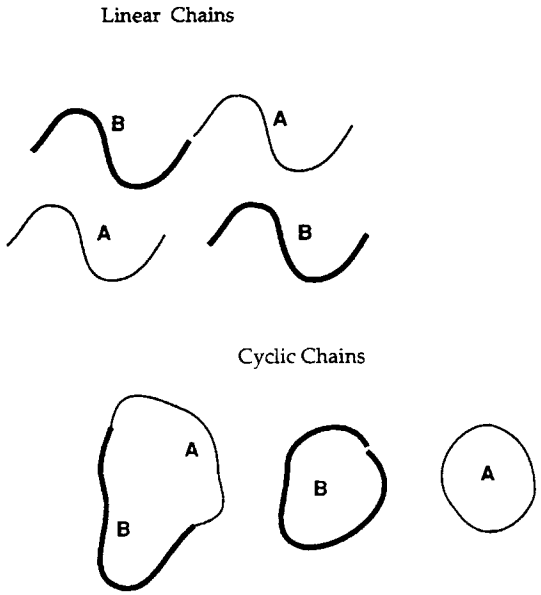

Fig. 2. Schematic representation of two mixtures of diblock copolymers AB and homopolymers A and B: One made with cyclic chains (see ref.[79]) and the other with linear chains (see ref.[81])

and B have approximately the same degree of polymerization which is 1/3 of the total degree of polymerization. The systems in Fig. 2 deal with 2 mixtures of copolymers AB and homopolymers A and B. The first system is made of all linear chains and is similar to the one investigated by Hashimoto et al.[81,82]. The second system is made of cyclic copolymers and homopolymers. The scattering properties and phase behavior of these mixtures are investigated and the results are compared to identify the effects of architecture.

3.1. Static scattering and phase behavior

The static scattering properties can be derived from the general result of the RPA (see Eq. (82)). In general for a mixture made of two monomer species A and B, the bare structure factors are given by Eqs. (37) to (39). For a mixture of homopolymers and block copolymers in solution, the structure matrix reads[80]

$$S(q)^{-1} = \begin{pmatrix} \frac{S_B^0}{\Delta S} + \nu_A & -\frac{S_{AB}^0}{\Delta S} + \nu_{AB} \\ -\frac{S_{AB}^0}{\Delta S} + \nu_{AB} & \frac{S_A^0}{\Delta S} \nu_B \end{pmatrix} \tag{87}$$

where ΔS *is* the determinant of the bare structure matrix. The partial structure factors $S_{AA}(q)$, $S_{BB}(q)$ and $S_{AB}(q)$ are obtained from the inversion of the above matrix. Letting $\Delta\nu$ be the determinant of the interaction matrix ν, one obtains:

$$S_{AA}(q) = \frac{S_A^0 + \nu_B \Delta S^0}{1 + \nu_A S_A^0 + \nu_B S_B^0 + 2\nu_{AB} S_{AB}^0 + \Delta\nu S^0} \tag{88}$$

$$S_{AB}(q) = \frac{S^0_{AB} + v_{AB}\Delta S^0}{1 + v_A S^0_A + v_B S^0_B + 2v_{AB}S^0_{AB} + \Delta v \Delta S^0} \tag{89}$$

$S_{BB}(q)$ can be obtained from Eq. (88) by interchanging the indices A and B and $S_{BA}(q) = S_{AB}(q)$ for symmetry reasons. The bare structure factors depend upon the type of system under investigation.

Linear triblock BAB and cyclic diblock ABB in a solvent

For a block copolymer which is similar to the one investigated by Amis et al., one has

$$S^0_A(q) = \varphi N f^2 P_A(q) \tag{90}$$

$$S^0_B(q) = \varphi N (1-f)^2 P_B(q) \tag{91}$$

$$S^0_{AB}(q) = \varphi N f(1-f) P_{AB}(q) \tag{92}$$

where for convenience, the subscript of the copolymer has been deleted and f represents its composition $f = N_A/(N_A + 2N_B)$. Combining these results yields:

$$\frac{S_{AA}(q)}{f^2 \varphi N} = \frac{P_A + v_B(1-f)^2 \varphi N \Delta P}{D} \tag{93}$$

$$\frac{S_{BB}(q)}{(1-f)^2 \varphi N} = \frac{P_B + v_A f^2 \varphi N \Delta P}{D} \tag{94}$$

$$\frac{S_{AB}(q)}{f(1-f)\varphi N} = \frac{P_{AB} - v_{AB} f(1-f)\varphi N \Delta P}{D} \tag{95}$$

$$D = 1 + v_A \varphi f^2 N P_A + v_B \varphi (1-f)^2 N P_B + 2v_{AB}\varphi f(1-f) N P_{AB} + f^2(1-f)^2 N^2 \varphi^2 \Delta v \Delta P \tag{96}$$

The architecture of the copolymer is inherent in the form factors P_A, P_B and P_{AB} which are specified below for a linear triblock BAB and a cyclic diblock ABB.

Linear triblock BAB

Calling $R_g = N\sigma^2/6$ the total radius of gyration, one has

$$P_A = \frac{2}{u_A^2}(e^{-u_A} + u_A - 1) \tag{97}$$

$$P_B = \frac{2}{u_B^2}(e^{-u_B} + u_B - 1) + \frac{e^{-u_A}(1 - e^{-u_B})^2}{2u_B^2} \tag{98}$$

$$P_{AB} = \frac{(1 - e^{-u_A})(1 - e^{-u_B})}{u_A u_B} \tag{99}$$

where for Gaussian unperturbed chains $u_A = fu$, $u_B = (1 - f)u$ and $u = q^2 N\sigma^2/6$.

Cyclic diblock ABB

Retaining the same definitions for the symbols as in the case of linear chains, one has the following form factors for the corresponding cyclic diblock ABB

$$P_A = \frac{f - 1/2}{f^2} C[u, (1/2 - f)\sqrt{u}] + \frac{1 - f}{f} H[uf(1 - f)] \tag{100}$$

$$P_B = \frac{1/2 - f}{(1 - f)^2} C[u, (f - 1/2)\sqrt{u}] + \frac{f}{1 - f} H[uf(1 - f)] \tag{101}$$

$$P_{AB} = \frac{1}{2f(1 - f)} \{C[u, 0] - f^2 P_A - (1 - f)^2 P_B\} \tag{102}$$

where $H[x]$ and $C[u, v]$ are defined as follows:

$$H[x] = \frac{1 - e^{-x}}{x} \tag{103}$$

$$C[u, v] = \frac{2e^{-u/4}}{\sqrt{u}} \int_v^{\sqrt{u/4}} dt\, e^{t^2} \tag{104}$$

One can write the scattered intensity in the form of the Zimm equation from which one can deduce an apparent second virial coefficient A_{2app} and an apparent radius of gyration R_{gapp}. The result is

$$\frac{(a - b)^2 c_A}{I(q)} = \frac{1}{S_{AA}(q)} = \frac{1}{M_{Aapp}} + 2A_{2app} c_A + \frac{q^2 R_{gapp}^2}{3M_{Aapp}} \tag{105}$$

with $c_A = fc$, $M_{Aapp} = fM$ and A_{2app} and R_{gapp} are given by:

$$A_{2app} = A_{2A}[f^2 + \alpha(1-f)^2 + 2\beta f(1-f)] \tag{106}$$

$$\alpha = A_{2B}/A_{2A} \qquad \beta = A_{2AB}/A_{2A} \tag{107}$$

One could also write the expression of the radius of gyration which depends upon the chain architecture. The details are given in refs.[79] and [80] where it is shown that by choosing $\alpha = 5$, $\beta = 3.1$, $A_{2A} = 10^{-4}$ cm^3/g^2 and $M = 4\ 10^4$ g/mol, one finds a good agreement between the theoretical results and the data of Amis et al.

Mixtures of homopolymers A and B and a diblock copolymer AB

This study was prompted by the work of Hashimito et al.[81,82] who studied the scattering properties and phase behavior of mixtures of linear diblock copolymers AB and linear homopolymers A and B. They discussed the interplay between macrophase and microphase separation transition when the concentration of copolymer is changed. When a certain amount of copolymer AB is added to a phase separated blend of A and B homopolymers, there is an effect of compatibilization and the blend becomes homogeneous. Nevertheless, if the amount of copolymer added is high enough, one may observe a microphase separation transition (MST) which can be monitored by the probing radiation by observing the evolution of the scattering with q. This MST is signaled by an infinite scattered intensity at $q^* = 2\pi/\lambda^*$, where λ^* is the wavelength of the "major" mode of fluctuations which drives the system unstable. Within the RPA, the scattered intensity in the one phase region is:

$$\frac{(a-b)^2}{I(q)} = \frac{S_A^0 + S_B^0 + S_{AB}^0}{S_A^0 S_B^0 - S_{AB}^{02}} - 2\chi \tag{108}$$

Since the mixture is made of homopolymers A and B and a copolymer AB, the bare structure factors are the same as in Eqs. (37) to (39). Similar studies have been reported on linear and cyclic chain systems. Formally, the equations written above are valid regardless of the chain architecture. For example, for linear chains, P_A and P_B are given by the Debye function and P_{AB} is:

$$P_{AB} = H[u_A]H[u_B] \tag{109}$$

with $u_A = fu$ and $u_B = (1-f)u$ and $u = q^2\,(N_{CA} + N_{CB})\sigma^2/6$. For cyclic chains, the form factor of a cyclic homopolymer is given by the Casassa function[83]

$$P_{HA} = C[u_A, 0] = \frac{2e^{-u_A/4}}{\sqrt{u_A}} \int_0^{\sqrt{u_A/4}} dt e^{t^2} \tag{110}$$

and the same form holds for P_{HB} changing the subscript A into B. For the cyclic diblock, P_{CA}, P_{CB} and P_{CAB} have a different form and were reported earlier in terms

of the function $C[u, v]$. Fig. 3 shows the variation of $N_C[S_A^0 + S_B^0 + 2S_{AB}^0]/[S_A^0 S_B^0 - S_{AB}^{02}]$ as a function of q for different values of the volume fraction of copolymer φ_C. From the top to the bottom curves, φ_C varies from 1 to 0.4. The continuous lines represent the results for the mixtures of cyclic chains whereas the dotted lines correspond to the linear chain system. The latter results are consistent with those reported by Hashimoto and coworkers. Starting from the top curves one notes that the minimum for the linear copolymer is much lower than that of the cyclic copolymer and its location q^* is smaller. This means that fluctuations of cyclic copolymers are damped significantly as compared to those of the linear copolymer and their wavelength is smaller. The critical interaction parameter for microphase separation is much smaller for the linear copolymer but the size characteristic of this microphase is much smaller for the cyclic one. There is an enhanced

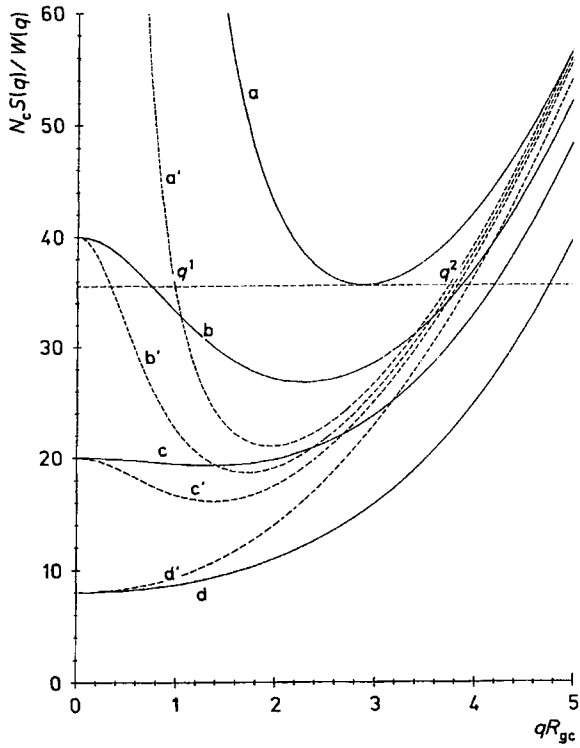

Fig. 3. Representation of $N_C[S_A^0 + S_B^0 + 2S_{AB}^0]/[S_A^0 S_B^0 - (S_{AB}^0)^2]$ as a function of qR_{gc} for different values of the volume fraction of copolymer φ_C, where $S(q) = [S_A^0 + S_B^0 + 2S_{AB}^0]$ and $W(q) = [S_A^0 S_B^0 - (S_{AB}^0)^2]$. The curves a, b, c, d correpond to the results for cyclic chains and $\varphi_C = 1$, 0.8, 0.6 and 0.4, respectively. The curves a', b', c', d' correspond to the results for linear chains and the same values of φ_C. The subscripts H and C stand for homopolymer and copolymer, respectively; A and B are the monomer species. In plotting the curves, we used $N = N_{AH} = N_{BH} = N_C/2$ for the degrees of polymerization and $R_{gHA}^2 = R_{gHB}^2 = R_{gC}^2/2$ for the radii of gyration (see Eq. (108))

compatibility towards microphase separation transition for the system of cyclic copolymers. Adding homopolymers A and B to this system, reduces the miscibility gap between linear and cylic chains. The minimum is lowered and shifted to the left for both systems. For example, curves d and d′ corresponding to $\varphi_C = 0.4$ are very close to each other for q from 0 to roughly $2/R_g$. For q above $2/R_g$, the effect of homopolymer architecture is more relevant. Below $\varphi_C = 0.4$, the curves present no minimum and the fundamental mode of fluctuations is the one for which $q \approx 0$. When the temperature is decreased, the first system to undergo MST is the one with linear chains which means that for a system showing an UCST (upper critical solution temperature), the critical temperature is lowered due to the cyclic architecture of the copolymer.

The spinodal equation which gives the critical interaction parameter can be obtained by letting the inverse scattering intensity go to zero at q^*. For a macrophase $q^* = 0$ and for a microphase transition q^* is finite. The result is:

$$2N_C\chi_S = \frac{N_C[S_A^0(q=q^*) + S_B^0(q=q^*) + 2S_{AB}^0(q=q^*)]}{[S_A^0(q=q^*)S_B^0(q=q^*) - S_{AB}^0(q=q^*)^2]} \tag{111}$$

q^* is obtained by minimizing the quantity $I(q)^{-1}$. The phase behavior of these mixtures is better illustrated in Fig. 4 which shows the variation of $2N_C\chi_S$ as a function of $\varphi = \varphi_{HA}/[\varphi_{HA} + \varphi_{HB}]$ for two values of φ_C. These curves show the spinodal lines for microphase and macrophase separation for both the linear (dotted lines) and cyclic (continuous lines) polymer mixtures as defined by Eq. (111). The misci-

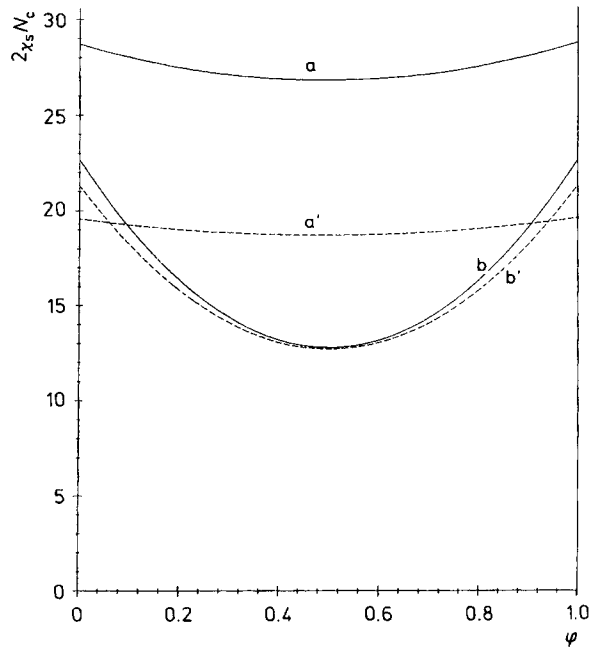

Fig. 4. Representation of the normalized critical parameter for microphase separation transition $2\chi_S N_C$ as a function of the composition in homopolymer A denoted $\varphi = \varphi_{HA}/(\varphi_{HA} + \varphi_{HB})$ for two values of the copolymer volume fraction φ_C. The continuous curves represent the results for cyclic chain sytems and the dashed curves the results for the linear chain systems. The curves a, a′ are plotted for $\varphi_C = 0.8$ and the curves b, b′ correspond to $\varphi_C = 0.4$ (see Eq. (111))

bility gap between the systems with cyclic and linear copolymers is quite large. This gap is reduced significantly when φ_C decreases and the volume fraction of homopolymers increases. In curves b and b′ for which $\varphi_C = 0.6$, this gap is very small, and for $\varphi_C = 0.4$, it is practically zero. In the latter case, the microphase is transformed into a macrophase separation transition since the fluctuating mode governing this phase separation has infinitely long wavelength. There is no major mode of fluctuation driving the system unstable with finite wavelength. This aspect is discussed in more details in ref.[79].

One should mention that the present results are consistent with the theoretical work of Markos and Rabin[84,85] on cyclic diblock copolymers in the bulk based on the method of Edward's Hamiltonian. Kosmas, Benoit and Hadziioannou[86] studied theoretically within a model similar to the one exposed here the scattering by cyclic homopolymers and copolymers at large wavevectors q. They found that for large N, linear and cyclic copolymers have the same behavior. Furthermore the same formalism designed to study linear polymers at large wavevectors can also be used for cyclic chains. Of course, there are many other theoretical studies of cyclic homopolymers and copolymers and it is beyond the scope of the present paper to review all of them. We have not reviewed in particular those investigations using more sophisticated models such as renormalization group theory methods or nonlinear higher order vertex functions[87] which are essential for the characterization of the ordered phases beyond the order-disorder transition temperature and which are more suitable to describe fluctuations and more subtle conformation changes than one can do with a simple RPA. This is not of course that these models are not interesting but, as we mentioned earlier, we would like to keep our discussions limited to simple cases for systems not subject to strong fluctuations.

To our judgment, the main drawback when examining the properties of cyclic homopolymers and copolymers is the lack of sufficient experimental data which could be used to test all these theories. We are well aware of the chemical difficulties to manifacture high molecular weight cyclic homopolymers and copolymers but we still hope that the chemists can feel the need and have enough motivation to embark into this adventure. This section on cyclic copolymers is included here in this paper to stress once more the need for more experiments in this field and the strong need for the synthetic chemist to face the challenge.

3.2. Dynamic scattering

Dynamic scattering properties of linear copolymers and linear homopolymers have been studied by many authors[1,2,8,9,29,66–69]. Here we focus our attention upon the copolymers of Fig. 1 considered in the QELS study of Amis et al. in the presence of a low molecular weight solvent with A = PS, B = PDMS and cyclohexane is the solvent.

In general, the partial dynamic structure factors $S_{ij}(q, t)$ for a mixture of p polymers in a solvent are sums of p relaxation modes

$$S_{ij}(q,t) = \sum_{k=1}^{p} A_{ijk}(q)\,\mathrm{e}^{-\Gamma_k(q)t} \tag{112}$$

where $A_{ijk}(q)$ and $\Gamma_k(q)$ are the amplitudes and relaxation frequencies of the eigenmodes. In the case of the systems of Fig. 1, i and j run over A and B since $p = 2$. More precisely, one has:

$$S_{AA}(q,t) = A_{AA,S}\,\mathrm{e}^{-\Gamma_S(q)t} + A_{AA,F}\,\mathrm{e}^{-\Gamma_F(q)t} \tag{113}$$

$$S_{AB}(q,t) = A_{AB,S}\,\mathrm{e}^{-\Gamma_S(q)t} + A_{AB,F}\,e^{-\Gamma_F(q)t} \tag{114}$$

Similar expressions can be written for $S_{BB}(q,t)$ and $S_{BA}(q,\,t)$ by interchanging the subscripts A and B. The subscripts S and F are introduced in place of $k = 1, 2$ for the sake of convenience in the physical interpretation of the eigenmodes as slow and fast modes, respectively. Since we are interested primarely on the data of Amis et al., $\partial n/\partial c_{B=(PDMS/cyclohexane)} = 0$, and only the PS block scatters the light. One should focus on the partial structure factor $S_{AA}(q,\,t)$ whose amplitudes are

$$A_{AA,F} = A_F = \frac{S_{AA}(\Omega_{BB} - \Gamma_F) - S_{AB}\Omega_{AB}}{\Gamma_S - \Gamma_F} \tag{115}$$

$$A_{AA,S} = A_S = S_{AA} - A_{AA,F} \tag{116}$$

and frequencies are:

$$\Gamma_F = \Omega_{av} + \sqrt{\Omega_{av}^2 - \Delta\Omega} \tag{117}$$

$$\Gamma_S = \Omega_{av} - \sqrt{\Omega_{av}^2 - \Delta\Omega} \tag{118}$$

$$\Omega_{av} = \frac{\Omega_{AA} + \Omega_{BB}}{2} \quad \text{and} \quad \Delta\Omega = \Omega_{AA}\Omega_{BB} - \Omega_{AB}\Omega_{BA} \tag{119}$$

In these expressions, S_{ij} are the static structure factors and Ω_{ij} the elements of the first cumulant matrix Ω. The former were written explicitely for the systems of Figs. 1 and 2 and the elements of the first cumulant matrix are

$$\Omega_{AA} = D_A^0 q^2 \frac{P_B + \nu_A f^2 \varphi N \Delta P}{f \Delta P} \tag{120}$$

$$\Omega_{AB} = -D_B^0 q^2 \frac{P_{AB} - \nu_{AB} f(1-f)\varphi N \Delta P}{(1-f)\Delta P} \tag{121}$$

where hydrodynamic interaction has been neglected. Note that the other two components Ω_{BB} and Ω_{BA} are deduced from the above equations after interchanging the subscripts A and B and changing f into $1 - f$. In the Rouse limit, the single chain diffusion coefficients D_0^A and D_0^B are:

$$D_0^A = k_B T/(N_A \zeta_A) \quad \text{and} \quad D_0^B = k_B T/(N_B \zeta_B) \tag{122}$$

To illustrate these results, we represent in Fig. 5 the variation of the normalized eigenfrequencies $\Gamma_{S,F}(q^2 D_0)$ as a function of $u = q^2 R_g^2$ for the systems of Fig. 1. Here, we assume that the single chain diffusion coefficients are equal to D_0. The insert in this figure represents the variation of the normalized amplitudes $A_S/(\varphi N)$ as a function of u for the same mixtures. The continuous curves are the results for the

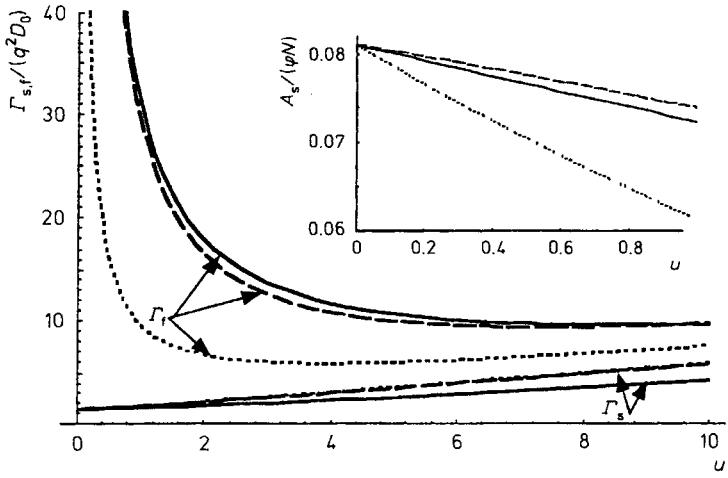

Fig. 5. Representation of the normalized eigenfrequencies for the slow and fast modes $\Gamma_{s,f}/(q^2 D_0)$ as a function of $u = q^2 R_g^2$ for the copolymers of Fig. 1 (see Eqs. (117) and (118)). The insert represents the normalized amplitude for the slow mode only, $A_s/(\varphi N)$, as a function of u for the same copolymers (see Eq. (116)). The continuous curves give the result for the cyclic diblock, the dashed curves are those of the linear triblock. In these plots, we have added, for comparison, the results of the linear diblock similar to the cyclic copolymer without one AB junction (dotted curves)

cyclic copolymer ABB whereas the dashed curves represent the results for the linear triblock BAB. We have included the results for the linear diblock ABB (dotted curves) for completeness which is similar to the cyclic copolymer in which one of the two bounds AB is released. In plotting these curves we have used the values $f = 1/3$, $2A_2Mc = 0.1$, $\alpha = A_{2B}/A_A = 5$ and $\beta = A_{2AB}/A_{2A} = 3.1$. The latter value uses in addition to $\alpha = 5$ an interaction parameter such that $\chi = A_{2A}/10$. In obtaining β, we have used the relationship between A_{2AB} and A_{2A} and A_{2B}[79,80].

$$A_{2AB} \approx \frac{1}{\varphi_S} - \chi_{AS} - \chi_{BS} + \chi \approx \frac{A_{2A} + A_{2B}}{2} + \chi \tag{123}$$

One observes a small difference between the frequencies of the structural mode in this range of q. This difference vanishes at higher q's. Γ_F of the linear diblock (dotted curve) is clearly distinct from the other two. Γ_S seems to be the same for the two linear copolymers. The difference to the cyclic copolymers increases with q. For the slow mode, at small q, the effect of architecture is not apparent but as q increases, the difference in the relaxation of the slow mode becomes more apparent due to the architecture of cyclic and linear chains partly because of the difference in R_g's. The difference between the amplitudes of the cyclic and triblock coolymers increases with q but the linear diblock shows a large difference to both of them at small q's. the slow mode is the only one appearing at $q \approx 0$ since its relative amplitude is 100% and decreases with q whereas A_F increases. The two amplitudes of the linear diblocks are found to cross each other at a much lower q and above this crossing point, the fast mode dominates the dynamics of the copolymer solution[8].

4. Networks and crosslinked blends

4.1. Free chains in a network

Combining rubber elasticity and Flory-Huggins lattice theory, Briber and Bauer derived the free energy for a network A and free chains B[14]:

$$\frac{f}{k_B T} = \frac{3A}{N_C}(\phi_S^{2/3}\varphi^{1/3} - \varphi) + \frac{B\varphi}{N_C}\ln\frac{\varphi}{\phi_S} + \frac{1-\varphi}{N_B}\varphi\ln(1-\varphi) + \chi(1-\varphi) \tag{124}$$

This is the free energy per unit volume, and the molar volumes of the network and the free chain are set to 1 for convenience. Φ_S denotes the volume fraction when the network is relaxed (reference state of the network), φ is the volume fraction of the network, N_C and N_B are the average number of monomers between crosslinks and the degree of polymerization of the free chains, respectively. A and B are constants equal to 1/2 and $2/f'$ (f') = functionality of crosslinks), respectively. This is an extreme case of a crosslinked blend A/B with only AA crosslinks and no AB or BB crosslinks. It shows drastic differences to networks where AB and BB crosslinks are dominant. The second derivative of the free energy with respect to φ gives the forward structure factor:

$$\frac{1}{S(q=0)} = \frac{2A\phi_S^{2/3}}{N_C\varphi^{5/3}} + \frac{B}{N_C\varphi} + \frac{1}{N_B(1-\varphi)} - 2\chi \tag{125}$$

Introducing the critical parameter for spinodal decomposition χ_S, one has:

$$\begin{aligned} \frac{1}{S(q=0)} &= 2(\chi - \chi_S) \\ \chi_S &= \frac{A\phi_S^{2/3}}{N_C\varphi^{5/3}} + \frac{B}{2N_C\varphi} + \frac{1}{2N_B(1-\varphi)} \end{aligned} \tag{126}$$

Briber, Lin and Bauer[88] investigated the collapse of free chains B in the network A and found three regimes. (i) For $N_C < N_B$, they found that the radius of gyration of free chains R_{gB} is the same as in the uncrosslinked melt. (ii) For $N_C < N_B$, the free chain undergoes shrinking since its radius of gyration decreases according to the law $R_{gB} \sim N_C$. A similar behavior is predicted by Muthukumar[89] for isolated chains in a field of random obstacles. (iii) For $N_C < N_B$, the free chains segregate. Muthukumar et al. found that when the density of obstacles is small, a transition from self avoiding to Gaussian behavior takes place. For a higher density of obstacles, a transition from Gaussian to the localized collapsed state occurs. R_{gB} scales with the density of obstacles as $R_{gB} \sim 1/N_C$.

The diffusion of free chains B in a network A is usually significantly slower as compared to the case where the matrix B is made of free polymer and $N_B \leq N_C$. The Harley-Crank equation for the diffusion coefficient gives[90]

$$D = [x_B D_A^0 + x_A D_B^0] \frac{\varphi_A \varphi_B}{x_A} \frac{\partial \mu_B}{\partial \varphi_B} \tag{127}$$

where x_A and x_B are the mole fractions of A and B polymers and μ_B is the chemical potential,

$$\mu_B = \frac{\partial \left(\frac{f}{k_B T}\right)}{\partial \varphi_B} \tag{128}$$

which using Eq. (124) yields:

$$\mu_B = \frac{A\phi_S^{2/3}(1-\varphi)^{1/3} - B(1-\varphi)}{N_C} + 1 - \varphi + \ln\varphi + \chi(1-\varphi)^2 \tag{129}$$

Fig. 6 represents the spinodal and coexistence curves as defined by Eqs. (126) and (129) where in the latter case the coexistence curve is obtained by letting $\mu_B = 0$. This phase diagram is slightly different from the usual one for a blend of free chains and describes the effects of the elasticity term of the network A.

For a crosslinked network at constant density, one has $D_A^0 = 0, \varphi = \varphi_B$ and the diffusion coefficient becomes:

$$D = D_B^0(1-\varphi)\varphi \frac{\partial \mu_B}{\partial \varphi} \tag{130}$$

$$D = -D_B^0(1-\varphi)\varphi N_B \left[\frac{A\phi_S^{2/3}(1-\varphi)^{-2/3}}{3N_C} - \frac{B}{N_C} - \frac{1-\varphi}{N_B\varphi} + 2\chi(1-\varphi)\right] \tag{131}$$

Including the effects of crosslinks in the elastic energy term reduces the diffusion coefficient and hence slows down the dynamics. One can study also the diffusion profile in the vicinity of the network and look at the penetration of the network by the free chains.

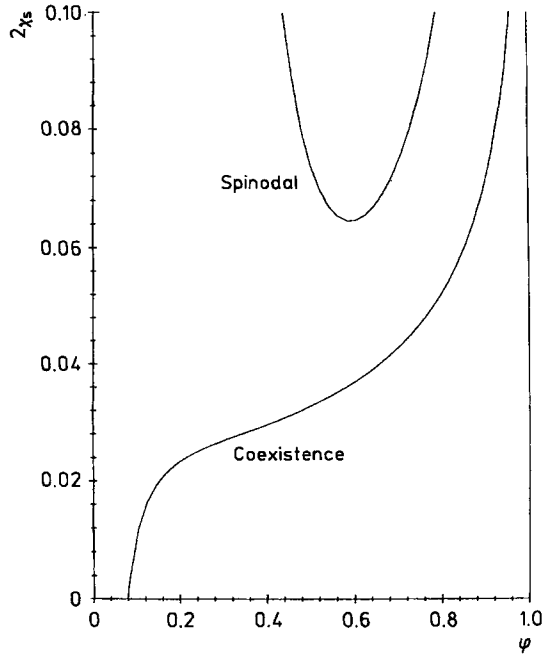

Fig. 6. Representation of the phase diagram for a network (A) and free chains (B) mixture. The lower curve is the coexistence curve obtained by equating the chemical potential in Eq. (129) to zero (see ref.[14]) and the upper curve is the spinodal line as defined by Eq. (126). The following values were used in these plots: $N_C = 500$, $N_B = 50$, $A = 1$, $B = 1/2$

Once again, we would like to stress the fact that the list of references given here on this subject is not complete and only few of them arbitrarily chosen are cited.

4.2. Crosslinked blends: de Gennes analogy

The generalization of the theory of multicomponent mixtures to crosslinked networks is not easy and requires a reformulation of the RPA to account for the crosslinks. To overcome this difficulty in the case of blends, de Gennes[40] proposed an analogy with charges in dielectric media. Using the fact that charges of opposite signs create local polarizations inducing attractive forces, de Gennes compared these forces with the elastic restoring forces characterizing the network. These forces produce enhancement of compatibility and since the two homopolymers A ane B are linked together, the phase separation in the thermodynamic limit of $q = 0$ cannot take place. Instead, a microphase separation transition (MST) is observed when the temperture reaches the critical value T_S. Fig. 7 gives a phase diagram which illustrate this enhancement of compatibility and a change from the macrophase transition in the blend of free chains to a microphase transition when the blend is crosslinked via AB junctions. This behavior can also be observed in scattering experiments whereby the scattered intensity exhibits a peak at $q = q^*$ which diverges at $T = T_S$. Concentration fluctuations have large amplitudes, long wavelength $\lambda^* = 2\pi/q^*$ and their relaxation time is infinitely long.

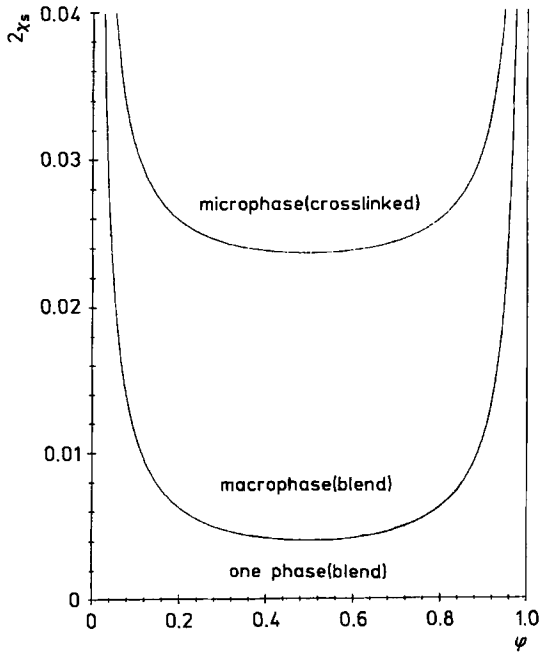

Fig. 7. Representation of the spinodal curves for macrophase separation of a blend A/B (lower curve) and for microphase separation of the corresponding crosslinked network (with A-B crosslinks only, upper curve). This phase diagram is given to illustrate the compatibility enhancement towards phase separation and due to the A-B crosslinks (see ref.[40])

Including the elasticity term due to restoring forces of the crosslinked blend, de Gennes obtained the structure factor as:

$$S^{-1}(q) = \frac{\chi_0 - \chi}{2} + \frac{q^2\sigma^2}{24} + \frac{C}{q^2} \tag{132}$$

where χ_0 is the critical parameter for macrophase separation of the blend of free chains in the RPA scheme:

$$2\chi_0 = \frac{1}{\varphi_A N_A} + \frac{1}{\varphi_B N_B} \tag{133}$$

C is the elastic constant of the crosslinked blend which has been obtained by de Gennes in terms of the number of monomers between crosslinks N_C as:

$$C = \frac{36}{N_C^2\sigma^2} \tag{134}$$

$S(q)$ admits maximum at $q = q^*$ which can be obtained by equating the derivative $dS(q)/dq$ to zero:

$$q^* = \frac{5.42}{N_C^{1/2}\sigma} \tag{135}$$

Fig. 8 shows the variation of $S(q)$ as a function of q for sevral values of the interaction parameter χ shown on this figure and $\chi_0 = 0$. As the χ parameter increases, the peak height increases and diverges at the critical value $\chi_S = 0.0098$. Its location q^* however does not shift with the temperature as indicated by Eq. (135). Assuming that crosslinking is made by γ-ray irradiation, Eq. (135) means that q^* is proportional to the square root of the radiation dose[14]. Equating $S^{-1}(q = q^*)$ to zero yields the critical parameter for MST:

$$\chi_S = \chi_0 + \frac{4.9}{N_C} \tag{136}$$

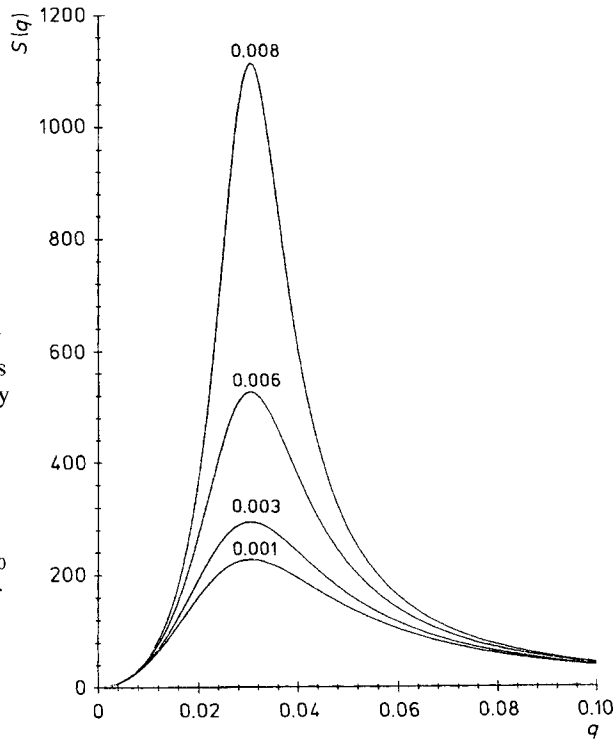

Fig. 8. Representation of the scattering curve $S(q)$ as a function of q predicted by de Gennes' model (see Eq. (132)) for several values of the c-parameter as indicated on the curves. The following parameters were used in these plots: $\chi_0 = 0$, $\sigma = 8$ Å and $N_C = 500$. Note that the critical parameter for MST has the value $\chi_S = 0.0098$

This is in qualitative agreement with the SANS data of Briber and Bauer[14] on dPS/PVME crosslinked blend although, instead of 5.42 in Eq. (135), the data gives 2.3. Moreover, the scattering at $q = 0$ is found to be finite unlike the Gennes' model which precticts $S(q = 0) = 0$. This discrepancy requires a generalization of the above model to improve the agreement with the data. There are several ways to generalize de Gennes model and improve the agreement with the experimental behavior. We shall not examine all the possiblities suggested in the literature and we content ourselves with one or two examples using the concept of frozen fluctuations at the temperature of crosslinking as first suggested by Briber et al.[14,88] and later used by Betachy et al.[91,92]

4.3. Extension of de Gennes' model

Briber and Bauer performed SANS experiments on uncrosslinked and crosslinked mixture of dPB/PB with $N_C = 38$ at temperatures varying between zero and 150 °C[14,32]. They have shown that (i) for uncrosslinked blends, the intensity increases substantially with T and the interaction parameter varies with temperature as ($T_S = 99.2$ °C):

$$\chi = -\frac{0.314}{T} - 5.34 \tag{137}$$

In this regard, it is interesting to note that the uncrosslinked blend of dPS/PVME has a LCST and its interaction parameter χ is found experimentallly to follow the law:

$$\chi = -\frac{20.6}{T} + 4.9 \times 10^{-2} \tag{138}$$

(ii) The intensity obtained by SANS or dPB/PB (polybutadiene) is found to be independent of T for the crosslinked blend and does not show microphase separation transition even near 0 °C ($T_S = 99.2$ °C). To analyze this behavior, they assumed that the scattering signal after crosslinking is the sum of two terms:

$$I(q) = I_f(q) + I_c(q) \tag{139}$$

where $I_f(q)$ is a signal of frozen fluctuations at the moment of crosslinking which remains essentially constant independent of T. $I_c(q)$ is the scattering after crosslinking and they suggested to identify this contribution with de Gennes result. Analyzing data for the crosslinked and uncrosslinked systems following a temperature jump from 105 to 150 °C, they found three distinct regions limited by q_1 and q_2: At $q < q_1$, the intensity of the crosslinked network is higher than that of the free chains. Two competing mechanisms take place: the crosslinking reaction tends to freeze the concentration fluctuations with a certain rate and the thermal fluctuations tend to relax these fluctuations with a rate $\Gamma^{-1}(q) \sim q^2$. It seems that below q_1, the freezing mechanism is faster than the relaxation process.In the intermediate range $q1 < q < \mathbf{q}_2$, the scattering from the crossliked blend is weaker whereas at $q > q_2$ the scattering from the free chains and th ecrosslinked blend are the same.

A slightly different argument has been used to extend de Gennes model and make it consistent with the data at $q = 0$. It uses the same analogy proposed by de Gennes but includes the screening phenomenon[41,91]. This introduced a new characteistic length κ^{-1} equivalent to the Debye-Huckel screening length. To understand this, one writes the free energy functional per unit volume

$$\frac{\Delta F}{k_B T} = \int \frac{d^3 r}{\sigma^3} A \left\{ \frac{f[\varphi(r)]}{k_B T} + \frac{\sigma^2}{36 \varphi_A \varphi_B} |\nabla \varphi_A|^2 + \frac{F_{ex}[\varphi(r)]}{k_B T} \right\} \tag{140}$$

where $[\varphi(r)]$ is the Flory-Huggins free energy:

$$\frac{f}{k_B T} = \frac{\varphi_A \ln \varphi_A}{\varphi_A} + \frac{\varphi_B \ln \varphi_B}{\varphi_B} + 2\chi \varphi_A \varphi_B \tag{141}$$

$\nabla\varphi(r)$ is the gradient of $\varphi(r)$ and $F_{ex}(\varphi)$ the excess free energy which, in the case of a dielectric medium, is written in terms of the local electric field $\boldsymbol{E}$ and the dielectric constant ε as:

$$F_{ex} = \varepsilon |\boldsymbol{E}|^2 \tag{142}$$

In de Gennes' analogy, F_{ex} is written in terms of the polarization $\boldsymbol{P}$ and the rigidity constant C of the medium as:

$$F_{ex} = C |\boldsymbol{P}|^2 \tag{143}$$

Expressing this excess free energy in terms of Fourier components of the density fluctuations, one finds in the case of bare charges a q^{-2} behavior whereas in the case of screened charges, one observes a $[q^2 + \kappa^2]^{-2}$ behavior which is reminescent of the long range screened correlations $e^{-\kappa r}/r$. This leads to the modification of Eq. (132) into the form:

$$S^{-1}(q) = \frac{\chi_0 - \chi}{2} + \frac{q^2 \sigma^2}{24} + \frac{C}{q^2 + \kappa^2} \tag{144}$$

κ^{-1} is the counterpart of the Debye screening length which for weakly crosslinked networks is identified as the end-to-end chain length:

$$\kappa^{-2} = N\sigma^2 \tag{145}$$

This analogy can also be extended to blends in the presence of a low molecular weight solvent. For arbitrary crosslinking densities, Bettachy et al.[32] proposed a model which combines de Gennes' analogy and the identification of the pseudo-screening length κ^{-1} with the correlation length of the frozen fluctuations at the temperature of crosslinking T_i. They defined κ in terms of T_i and T_j the temperature to which the system is driven after crosslinking. In de Gennes' initial model, it is implicitely assumed that the initial temperature T_i is infinite and the blend is completely homogeneous. Bettachy et al. assumed that the scattering at $q = 0$ remains the same before and after crosslinking. By equating the scattered intensity for the blend of free chains at $T = T_i$, i.e., S^{-1} ($q = 0$, free chains) = 2 ($\chi_0 - \chi_i$), to the forward scattering intensity for the crosslinked blend at T_f, i.e., S^{-1} ($q = 0$, crosslinked) = 2 ($\chi_0 - \chi_i$) + C/κ^2, one obtains the characteristic length κ^{-1}:

$$\kappa^2 \approx \frac{C}{\chi_f - \chi_i} \tag{146}$$

Since $C \sim N_C^{-2}$, one finds tht κ^{-1} is proportional to the average distance between crosslinks. For weakly crosslinked networks, $N_C \sim N$ and one recovers the earlier result. The position of the maximum q^* is also dependent upon κ and C:

$$q^{*2} \approx \frac{\sqrt{C}}{\sigma} - \kappa^2 \tag{147}$$

The effect of initial frozen fluctuations is to shift q^* to smaller values implying a reduction in the sharpness of the scattering peak and the microphase structure. There is an enhancement of compatibility towards MST taking place at the critical parameter where $S^{-1}(q = q^*) = 0$:

$$\chi_S = \chi_0(\text{blend}) + \frac{2C}{q^{*2} + \kappa^2} \tag{148}$$

χ_S is increased by a quantity proportional to $\sqrt{C}$ when the crosslinking effect is included.

4.4. Charged blends with crosslinks

For simplicity, we choose the case where polymer A is charged and B neutral and assume that f^{-1} monomers separate two charges e along a chain A[91]. The static structure factor $S(q)$ becomes:

$$S^{-1}(q) = S_0^{-1}(q) + \frac{c}{q^2 + \kappa_g^2} + \frac{c_d}{q^2 + \kappa_d^2} \tag{149}$$

The difference to the case of neutral networks is given by the last term in this equation which contains the new rigidity constant c_d. The similarity between the electrostatic term and the network elasticity contribution is a clear illustration of the analogy suggested by de Gennes. The only distinction is in the rigidity constants C's and the screening lengths κ's which have different origins and depend upon different parameters; c_d depends on the charge parameter f and the Bjerrum length $l = \frac{e^2}{\varepsilon k_B T}$ as follows

$$c_d = \frac{4\pi l f^2}{\sigma^3} \tag{150}$$

where ε is the dielectric permittivity, k_B the Boltzman constant.

$$\kappa_d^2 = \frac{4\pi l}{\sigma^3}(\varphi_{ci} + \varphi_{salt}) \tag{151}$$

The volume fraction of counterions ϕ_{ci} is equal to $xf\phi$ because of electroneutrality and ϕ_{salt} is the added salt concentration. The electrostatic term in Eq. (149) implicitly means that the Debye-Hückel model has been used for point-like charged particles on the polymer network. This approximation is perhaps too crude but it helps to keep the formalism at a fairly simple level without, in our opinion, loosing the main features of the effects of long range electrostatic interactions.

The Debye-Hückel approximation provides a reasonable description of interaction

between point-like particles at long distances where other interactions of much shorter ranges such as hard sphere or Van der Waals interactions are weaker. Obviously, one could improve quantitatively the electrostatic description by using other models such as the Poisson-Boltzmann equation but this introduces additional numerical complications without a real gain into the physical insight of the charged network problem.

Eq. (149) shows tht depending upon the relative values of the characteristic quantities C's and κ's, the scattering behavior is either dominated by the crosslinks or the charges. In some cases, it may however be difficult to distinguish these contributions and evaluate them separately. One can consider three cases.

a: $\kappa_d = \kappa_g = \kappa$

In this case, the density of crosslinks, the ionic strength and f are tuned in such a way that:

$$\frac{4\pi l}{\sigma^3}(\phi_{ci} + \phi_{salt}) = \frac{n}{N}\,\frac{1}{n^{2\nu}\sigma^2} \tag{152}$$

$$\phi_{ci} + \phi_{salt} = \frac{1}{4\pi}\,\frac{1}{l/\sigma}\,\frac{1}{N/n}\,\frac{1}{n^{2\nu}} \tag{153}$$

l/σ is proportional to Manning's parameter, N/n is the number of crosslinks per chain. The volume fraction in Eq. (153) is proportional to $1/N$ and may be quite small. In a theta solvent, it is independent of the crosslink density n and decreases as $n^{-0.66}$ in a good solvent. In the latter case, the chains are swollen inside the network pore and therefore the concentration of counterions is higher implying that the screening is more effective as compared to a theta solvent. The electrostatic and the elasticity terms can be combined and one obtains:

$$S^{-1}(q) = S_0^{-1}(q) + \frac{c_{app}}{q^2 + \kappa^2} \tag{154}$$

$S_0^{-1}(q)$ is the bare structure factor and c_{app} the apparent rigidity constant:

$$c_{app} = c + c_d \tag{155}$$

The peak position of $S(q)$ shifts to lower values when c_{app} decreases as one can see from Eq. (147). There is substantial enhancement of compatibility towards macrophase separation and emergence of a peak at q_m as a result of combined elastic and electrostatic forces. By lowering the temperature, the interaction between A and B reaches a critical value χ_S at $T = T_s$ and the structure factor diverges at $q = q^*$:

$$\chi_S = \chi_0 + \chi_0 R_g^2 q^{*2} + \frac{c}{2(q^{*2} + \kappa_g^2)} + \frac{c_d}{2(q^{*2} + \kappa_d^2)} \tag{156}$$

The fluctuations with a wavelength in the vicinity of $\lambda^* = 2\pi/q^*$ are unstable and those with a wavelength outside this range are stable and describe the dynamics in the homogeneous one phase region.

b: $\kappa_d \gg \kappa_g$: Excess added salt

κ_d increases linearly with the square root of the added salt concentration resulting in a substantial weakening of Coulomb forces due to screening at distances exceeding κ_d^{-1}. In these conditions, the crosslinks determine the essential features of the phase behavior and scattering properties of the network. In excess salt, one recovers the behavior of neutral polymers.

c: $\kappa_d \ll \kappa_g$: No added salt

In the absence of added salt, the screening length is determined uniquely by the counterions released by the network itself. If the range of electrostatic interactions is long compared to the average distance between crosslinks, the Coulomb interactions produce the main effect governing the scattering properties and phase behavior of the network.

5. Conclusions

In this paper, the scattering properties and phase behavior of polymer blends, block copolymers and networks are investigated. The presence of stiff chains in the blend induces a liquid crystalline phase which is discussed on the basis of the nematic interaction only. Models developed by Doi, Hammouda and others using a generalization of the RPA are briefly reviewed. The compressibility problem is examined together with the free volume theories of Sanchez et al. and Hammouda et al. The effects of pressure are included along these lines and the condition under which coupling between density and composition fluctuations vanishes is shown.

The dynamics of copolymers in bulk and in solution lead to emergence of new modes which are not encountered in counterpart blends of homopolymers. These are the structural mode, the polydispersity mode and the aggregation diffusional mode. The case of cyclic homopolymers and copolymers and their mixtures is considered. The scattering and thermodynamic properties of these mixtures are compared with those of their counterpart made of linear chains only. Drastic differences are observed. The mixtures with cyclic chains are characterized by a much better compatibility than their linear counterparts. It is shown that an interplay between macrophase and microphase separation transitions exists in general but its implications are different whether chains are linear or cyclic.

The dynamics are also characterized by the bimodal analysis of slow and fast modes but the properties of these modes are highly sensitive to the cyclic architecture of the chain.

The presence of crosslinks in a blend is also discussed. Two systems are considered. The first one is a mixture of a network A and free chains B. Effects of the net-

work elasticity on the phase behavior are discussed using the model of Briber et al. A crosslinked blend in which A and B homopolymers are connected by permanent crosslinks is also considered. de Gennes' model in which the effects of crosslinks is compared with those of electric charges in a dielectric medium is also discussed. Consistently with experiments, this model predicts enhancement vis-à-vis the macrophase separation transition but the emergence of a microphase transition if the temperature of the crosslinked blend reaches a critical value. The extension of de Gennes model to include the effects of initial fluctuations at the temperature of crosslinking is discussed. This extension is motivated by the experimental observation that the scattering at $q = 0$ is finite different from zero unlike the de Gennes model which predicts that $S^{-1}(q) = 0$ at $q = 0$.

This work was initiated during a stay of M. Benmouna at the *University of Maryland, Department of Materials and Nuclear Engineering* and at the *NIST, Materials Science and Engineering Laboratory* (November 1995) and completed at the *Max-Planck-Institut für Polymerforschung*. He expresses his gratitude to Professor *E. W. Fischer* for his interest in this work and constant encouragements. This material is based upon activities supported by a *National Science Foundation (NSF)* grant to *NIST* (DMR-9122444). Identification of certain equipment or materials does not imply recommendation by the National Institute of Standards and Technology.

[1] J. S. Higgins, H. Benoit, *"Polymers and Neutron Scattering"*, Oxford Science Publications, Clarendon Press, Oxford 1994
[2] P. G. de Gennes, *"Scaling Concepts in Polymer Physics"*, Cornell University Press, Ithaca 1979
[3] J. E. Mark, B. Erman, *"Rubberlike Elasticity – A Molecular Primer"*, John Wiley, NY 1988
[4] T. A. Vilgis, in *"Comprehensive Polymer Science"*, Vol. 6, Pergamon Press, Oxford 1989, pp. 227ff.;
R. Holyst, T. A. Vilgis, *Macromol. Theory Simul.* **5**, 573 (1996)
[5] S. F. Edwards, T. A. Vilgis, *Polymer* **27**, 483 (1987)
[6] P. J. Flory, *"Principles of Polymer Chemistry"*, Cornell University Press, Ithaca 1965
[7] C. C. Han, in *"Studies in Polymer Science"*, Vol. 2, Elsevier Science Publishers, Amsterdam 1988, pp. 223ff.
[8] Z. A. Akcasu, G. Nägele, R. Klein, *Macromolecules* **24**, 4408 (1991)
[9] Z. A. Akcasu, in *"Dynamic Light Scattering: The Method and some Applications"*, Oxford Science Publications, Oxford 1992, pp. 1ff.
[10] L. Leibler, *Macromolecules* **5**, 1283 (1982)
[11] G. R. Strobl, *Macromolecules* **18**, 558 (1985)
[12] G. Frederickson, *J. Chem. Phys.* **28**, 258 (1986)
[13] J. des Cloizeaux, G. Jannink, *"Les Polymères en Solution"*, Oxford University Press, Oxford 1990
[14] R. M. Briber, B. J. Bauer, *Macromolecules* **21**, 3296 (1988)
[15] B. Zimm, *J. Chem. Phys.* **4**, 164 (1946)
[16] L. Ould-Kaddour, *PhD Thesis,* Université Louis Pasteur, Strasbourg 1988
[17] L. Ould-Kaddour, C. Strazielle, *Polymer* **28**, 459 (1987); **33**, 899 (1992)
[18] P. Kratochvil, J. Vorlicek, D. Strakova, Z. Tuzar, *J. Polym. Sci., Polym. Phys. Ed.* **14**, 1561 (1976)

[19] L. Giebel, R. Borsali, E. W. Fischer, G. Meier, *Macromolecules* **23**, 4054 (1990)
[20] R. Borsali, M. Duval, M. Benmouna, *Macromolecules* **22**, 816 (1989)
[21] P. J. Davis, D. N. Pinder, P. T. Callagan, *Macromolecules* **5**, 170 (1992); 2**6**, 3381 (1993)
[22] M. R. Aven, C. Cohen, *Macromolecules* **23**, 476 (1990)
[23] J. Debrieres, R. Borsali, M. Rinaudo, M. Milas, *Macromolecules* **26**, 2592 (1993)
[24] T. Csiba, G. Jannink, D. Durand, R. Papoular, A. Lapp, L. Auvray, F. Boue, J. P. Cotton, R. Borsali, *J. Phys. I* **1**, 381 (1991)
[25] R. Borsali, H. Benoit, J. F. Legrand, M. Duval, C. Picot, M. Benmouna, B. Farago, *Macromolecules* **22**, 4119 (1989)
[26] M. Duval, C. Picot, R. Borsali, H. Benoit, M. Benmouna, C. Lartigue, *Macromolecules* **24**, 3185 (1991)
[27] H. Yamakawa, *"Modern Theory of Polymer Solutions"*, Harper and Row, NY 1971
[28] M. Olvera de La Cruz, I. C. Sanchez, *Macromolecules* **19**, 2501 (1986)
[29] B. Hammouda, *Macromolecules* **26**, 4800 (1993)
[30] M. Doi, S. F. Edwards *"The Theory of Polymer Dynamics"*, Oxford University Press, Oxford 1986
[31] P. G. de Gennes, *Physics* **3**, 37 (1967)
[32] E. Dubois-Violette, P. G. de Gennes, *Physics* **3**, 181 (1967)
[33] R. Pecora, *J. Chem. Phys.* **43**, 1562 (1965)
[34] Z. A. Akcasu, M. Benmouna, C. C. Han, *Polymer* **21**, 866 (1980)
[35] D. Richter, J. Hayter, R. Mezei, B. Ewen, *Phys. Rev. Lett.* **41**, 1484 (1978)
[36] M. Adam, M. Delsanti, *Macromolecules* **10**, 1227 (1977)
[37] R. Borsali, M. Duval, M. Benmouna, *Macromolecules 2***2**, 816 (1989)
[38] R. Borsali, M. Duval, M. Benmouna, *Polymer* **30**, 611 (1989)
[39] W. Brown, T. Nicolai, in *"Dynamic Light Scattering: The Method and some Applications"*, Oxford 1992, pp. 272 ff.
[40] P. G. de Gennes, *J. Phys. Lett.* **40**, 69 (1979)
[41] A. Bettachy, A. Derouiche, M. Benhamou, M. Daoud, *J. Phys. I* **1**, 153 (1991)
[42] H. Jinnai, H. Hasegawa, T. Hashimoto, R. M. Briber, C. C. Han, *Macromolecules* **26**, 182 (1993)
[43] H. Benoit, M. Benmouna, *Macromolecules* **17**, 535 (1984)
[44] W. H. Stockmayer, *J. Chem. Phys.* **18**, 58 (1950)
[45] H. Benoit, W. L. Wu, M. Benmouna, B. Bauer, A. Lapp, *Macromolecules* **18**, 986 (1985)
[46] M. Duval, C. Picot, M. Benmouna, H. Benoit, *J. Phys. (France),* **49**, 1963 (1988)
[47] T. Hashimoto, K. Mori, *"SANS from block copolymers in disordered state III. Concentrated solutions under optically theta conditions"*, preprint
[48] M. Benmouna, B. Hammouda, *Adv. Polym. Sci.*, in press
[49] M. Doi, K. Okono, *J. Chem. Phys.* **88**, 2815 (1988)
[50] R. Holyst, M. Schick, *J. Chem. Phys.* **96**, 721 (1992)
[51] B. Hammouda, *J. Chem. Phys.* **98**, 3439 (1993)
[52] B. Hammouda, *Adv. Polym. Sci.* **106,** 89 (1993)
[53] M. Shimada, T. Doi, K. Okano, *J. Chem. Phys.* **88**, 718 (1988)
[54] T. Doi, M. Shimada, K. Okano, *J. Chem. Phys.* **88**, 4070 (1988)
[55] M. Shimada, T. Doi, K. Okano, *J. Chem. Phys.* **88**, 2815 (1988)
[56] N. J. Wagner, L. M. Walker, B. Hammouda, *Macromolecules* **28**, 5075 (1995)
[57] B. Hammouda, B. J. Bauer, *Macromolecules* **28**, 4505 (1995)
[58] S. Janssen, G. Meier, D. Schwahn, K. Mortensen, *Europhys. Lett.* **22**, 577 (1993)
[59] D. A. Hajduk, *"Morphological Transitions in Block Copolymers"*, PhD Thesis, Princeton University, 1994
[60] B. Hammouda, C. C. Lin, N. P. Balzara, *Macromolecules 2***8,** 4765 (1995)

61) B. Hammouda, M. Benmouna, *J. Polym. Sci., Part B: Polym. Phys.* **33**, 2359 (1995)
62) I. C. Sanchez, R. H. Lacombe, *J. Chem. Phys.* **86**, 2353 (1976)
63) U. Bidkar, I. C. Sanchez, *Macromolecules* **28**, 1145 (1995)
64) H. Benoit, *Polymer* **32**, 579 (1991)
65) J. des Cloizeaux, G. Jannink, *Physica A* **102A**, 1206 (1980)
66) Z. A. Akcasu, M. Benmouna, H. Benoit, *Polymer* **27**, 1935 (1986)
67) M. Benmouna, M. Duval, R. Borsali, *J. Polym. Sci., Polym. Phys. Ed.* **25**, 1839 (1987)
68) M. Benmouna, H. Benoit, R. Borsali, M. Duval, *Macromolecules* **20**, 2620 (1987)
69) Z. A. Akcasu, M. Benmouna, B. Hammouda, *J. Chem. Phys.* **80**, 2766 (1984)
70) T. A. Vilgis, R. Borsali, *Phys. Rev. A* **43**, 6857 (1991)
71) R. Borsali, E. W. Fischer, M. Benmouna, *Phys. Rev. A* **43**, 5732 (1991)
72) M. Duval, H. Haida, J. P. Lingelser, Y. Gallot, *Macromolecules* **24**, 6867 (1991)
73) T. Jian, S. H. Anastasiadis, A. N. Semenov, G. Fytas, G. Fleischer, A. D. Vilesov, *Macromolecules* **28**, 2439 (1995)
74) C. Pan, W. Maurer, Z. Liu, T. P. Lodge, P. Stepanek, E. D. Von Meerwall, H. Watanabe, *Macromolecules* **28**, 1643 (1995)
75) C. J. C. Edwards, R. F. T. Stepto, in "*Cyclic Polymers*", J. A. Selmyen, Ed., Elsevier, London 1986
76) M. Santore, C. C. Han, G. McKenna, *Macromolecules* **25**, 3416 (1992)
77) E. J. Amis, D. F. Hodgson, *Polym. Prep. (Am. Chem. Soc., Div. Polym. Chem.)* **32**, 617 (1991)
78) E. J. Amis, D. F. Hodgson, W. Wu, *J. Polym. Sci., Part B: Polym. Phys.* **31**, 2049 (1993)
79) M. Benmouna, A. Bensafi, S. Khaldi, *J. Polym. Sci., Part B: Polym. Phys.*, in press
80) M. Benmouna, H. Benoit, S. Khaldi, A. Bensafi, *Macromolecules*, to be published
81) H. Tanaka, T. Hashimoto, *Polym. Commun.* **29**, 212 (1988)
82) Y. Ijichi, T. Hashimoto, *Polym. Commun.* **29**, 135 (1988)
83) E. F. Casassa, *J. Polym. Sci., Part A:* **3,** 604 (1965)
84) J. F. Marko, *Macromolecules* **26**, 1441 (1993)
85) J. F. Marko, I. Rabin, *Macromolecules* **5**, 1503 (1992)
86) M. Kosmas, H. Benoit, G. Hadziioannou, *Colloid Polym. Sci.* **272**, 1466 (1994)
87) A. Weyersberg, T. Vilgis, *Phys. Rev. E* **49**, 4 (1994)
88) H. Lin, R. M. Briber, B. J. Bauer, *Science* **268**, 395 (1995)
89) M. Muthukumar, *J. Chem. Phys.* **90**, 4542 (1989)
90) H. Sillescu, *Makromol. Chem., Rapid Commun.* **5**, 519 (1984)
91) M. Benmouna, T. A. Vilgis, M. Daoud, M. Benhamou, *Macromolecules* **27**, 1172 (1994)
92) A. Bettachy, A. Derouiche, M. Benhamou, M. Benmouna, T. A. Vilgis, M. Daoud, *Macromol. Theory Simul.* **4**, 67 (1995)